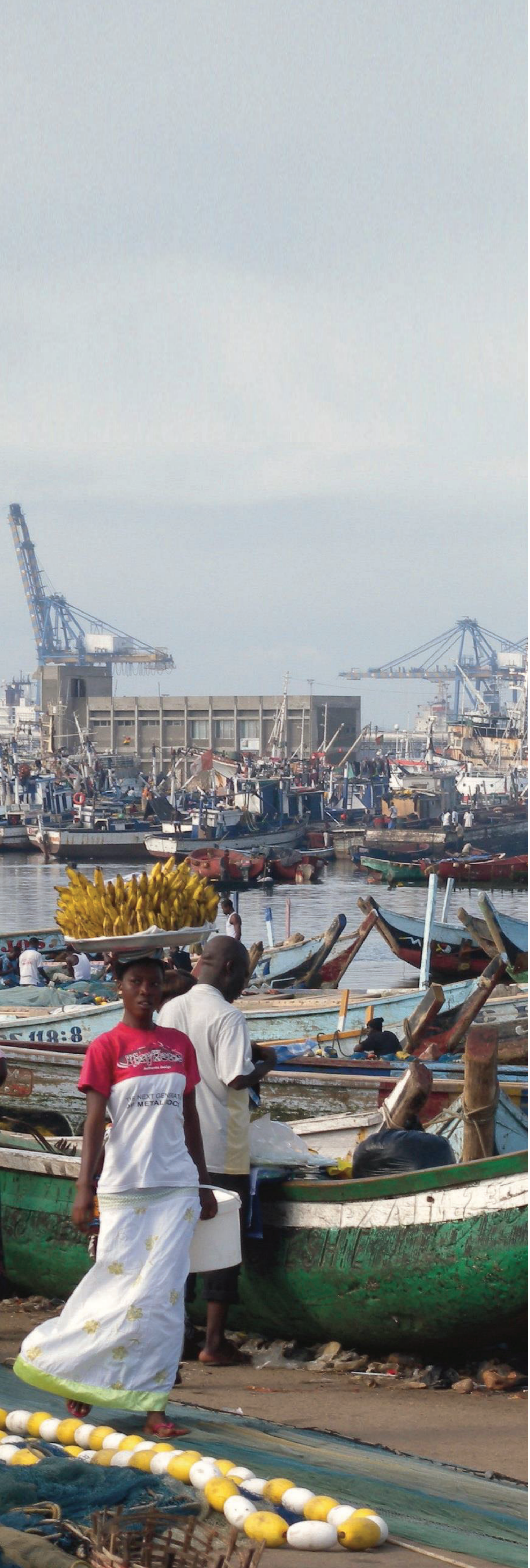

Universität Trier

Christel Weable

Analysis of Urbanization Patterns in the Densu Delta and Surrounding Areas (Accra, Ghana)

An Interdisciplinary Approach combining Remote Sensing and Human Geography Methods

WaterPower Working Paper Volume No. 20

WATERPOWER

WaterPower Working Paper Series

WaterPower Working Paper Series
ISSN (Print) 2510-0521
ISSN (Online) 2510-2222
Governance and Sustainability Lab
Faculty VI - Regional and Environmental Sciences
University of Trier

Suggested Citation: Weable, Christel (2019): Analysis of Urbanization Patterns in the Densu Delta and Surrounding Areas (Accra, Ghana) - An Interdisciplinary Approach combining Remote Sensing and Human Geography Methods. WaterPower Working Paper, No. 20. Governance and Sustainability Lab. Trier.

Authors' addresses

Christel Weable
C.Weable@t-online.de

Abstract

In the following research an interdisciplinary approach is taken to analyze urban growth in the Densu delta and its surrounding areas. Doing so, human geography and remote sensing knowledge were combined. The importance of interdisciplinary work is based on the fact that classifications of remotely sensed data, and presentation of any kind of data for that matter, always reflects the knowledge and priorities of the analyst. Therefore, to use results of remotely sensed data for urban science, including human geography, the analyst needs a better understanding of what the data can be used for, including what the data can not provide. Satellite data of the study area from the time frame 2008-2010 (mosaic image) and 2017 are classified using the machine learning technique random forest. A nested hierarchy classification scheme was used, resulting in five land cover classes on the first level: 'Bare Land', 'Vegetation', 'Urban', 'Tarmac' and 'Water'. The resulting classification has a of 0.82 from 2008-2010 and 0.79 for 2017. Over the course of almost a decade the urban land cover shows an annual growth rate of 3.11%, while vegetation decreases by 2.37% per year and bare land by 0.05%. To investigate differentiation of urban development the ratios of the three mentioned land cover classes per sq.km were plotted in a Ternary diagram. Distinguishable compositions for the two districts AMA and Ga South, which border in the study area, were detected. Plotting the composition of the three land covers is helpful to discriminate between different degrees of development. This study was by no means exhaustive, but the results suggest an interdisciplinary approach can be useful for human geography and urban studies through the use of remote sensing and machine learning classifications to describe urban phenomena.

Analysis of Urbanization Patterns in the Densu Delta and Surrounding Areas (Accra, Ghana)

An Interdisciplinary Approach combining Remote Sensing and Human Geography Methods

Christel Weable

1 Introduction 1

2 Theoretical Background 3

2.1 Debate about Land Cover Classification 3
2.2 Synopsis of Land Use Cover Change Applications 4
2.3 Conception of Patterns and Comparative Methodology 7
2.4 Accra, the Densu Delta and Surrounding Areas 10

3 Method 14

3.1 Data and Pre-processing of Imagery 14
3.2 Random Forest Classification 15
3.3 Accuracy Assessment 18
3.4 Land Cover Extents and Change 19
3.5 Pattern Detection 20

4 Results & Discussion 22

4.1 Accuracy of Classification 22
4.2 Urban Land Cover Growth in almost a Decade 24
4.3 Patterns of Urban Land Cover Growth 30

5 Conclusion and Outlook 36

Bibliography 38

A. Appendix 42

1 Introduction

Urbanization is a global driver and cities are rapidly growing in both size and number (UN Habitat, 2016; United Nations, 2016). "In 2016, an estimated 54.5% of the world's population lived in urban settlements" (United Nations, 2016). In other words, living in an urban environment now is the dominant way of living and these numbers are predicted to increase. One example is the prediction of Africa's urbanization level to reach about 58% in 2050, with urban areas on the continent hosting almost a quarter of the world's population (Cobbinah, Gaisie, & Owusu-Amponsah, 2015). In the process of cities gaining a more dominant role in the global economy as centers of both consumption and production as a result of rapid urbanization, challenges of supplying its citizens with the very basic services increase at an even higher speed, especially in the Global South[1] (Cohen, 2006). Hence the process of urbanization effects us in various ways, starting by health and living situation, over policy and security to food and environment, as well as climate change and many other topics. Therefore 'urbanization' has become an ubiquitous topic in many research fields.

Simone and Pieterse state in the book "New Urban Worlds" that 'urban knowledge' is located in a field between two axes (Simone & Pieterse, 2017). The first axis stretches from surface knowledge to in-depth understandings of highly localized phenomena. Surface knowledge is considered the knowledge which can be gathered from quantitative data sets, which allows the analyst to consider scale, frequency, rationalities and patterns over time, while in-depth understandings includes the understanding of psychological interiors of acting and drawing on relational ontologies. The second axis stretches between applied theoretical concerns (defined, in contradistinction to philosophy, aesthetics and the poetic, as 'grounded pragmatism'). Only through an ensemble of research between these axis is it possible to get closer to a true understanding of urbanism. Two research fields, which are connected to the generation of 'urban knowledge' are remote sensing and (human) geography. Each research field approaches the topic from a different perspective but overlap with regards to research of the spatial.

From a remote sensing approach, there are studies such as the "Atlas of Urban Expansion" (Angel, Blei, Parent, Lamson-Hall, & Sánchez, 2016) and "Global Urban Footprint" (German Aerospace Center, 2016) which map the urban extent of cities, as well as studies like the "National Land Cover Database" (Homer et al., 2015), which monitors land cover change of the United States in a long term. While these approaches are concentrated on *where* things happen and how to best extract information out of earth observation (EO) data, human geography is more

[1]The term 'Global South' is not used in this thesis as an exclusively, or strictly, geographical category. Instead it is meant as a social indicator including politically, environmentally and economically vulnerable communities (Pellow, 2007).

interested in *how* and *why* things happen in a spatial context. Therefore, human geography can approach the topic with studies in the same manner as "The production of uneven access to land and water in peri-urban spaces: *de facto* privatisation in greater Accra" (Bartels, Bruns, & Alba, 2018), where the control over and access to land and water in peri-urban spaces is discussed. Another example is "Incremental infrastructures: material improvisation and social collaboration across post-colonial Accra" (Silver, 2014), that deals with the subject of incremental infrastructures in relation to other subjects, e.g. the energy network. The variables of interest in these studies have a spatial extent, but are not measured from the air, therefore not visible in EO data. Often the visible human artifacts being buildings, crop fields and roads are less interesting than the abstract variables that explain their appearance and transformation. Land use change including construction of buildings, roads and the like are seen as manifestations of more important variables, for instance government policies, distributions of wealth and power, and social customs, none of which can be directly reflected in the bands of the electromagnetic spectrum (Rindfuss & Stern, 1998).

Hence integrating both approaches requires the combination of not only data, but also of quite different scientific traditions and views. "It is easy for scientists on one side to underestimate the difficulty of learning the approaches, theories, methods, and jargon of the other" (Rindfuss & Stern, 1998). This quote was stated in a book named "People and Pixels: Linking Remote Sensing and Social Science" back in 1998 and it still mostly stands today (Liverman, Moran, Rindfuss, & Stern, 1998). So the reason to link two different disciplinarians, in this case remote sensing and human geography, is to bring together knowledge from both disciplines, to build urban science (Acuto, Parnell, & Seto, 2018). As stated before, urban areas play an important role in many topics and yet "academia is lagging behind" (Acuto et al., 2018). Acuto et al. describes 'urban science' remaining trapped in the twentieth-century tradition of the systematic study of individual cities in specialized academic disciplines. In this thesis, an interdisciplinary approach is used for analyzing urbanization patterns in the Densu delta and surrounding areas in Accra, Ghana, combining remote sensing and human geography methods. The Densu delta and surrounding areas are the center of this research, since previous research including field work in Accra has been conducted there. In the corresponding Research Project two streets in the Densu delta were analyzed using mapping keys (Weable, 2018).

In the following chapter the theoretical background about the state of the art is presented followed by the introduction of the study site. Subsequently the methods used are explained. This is followed by the results and the simultaneous discussion of the former. Rounding off the thesis, the conclusion summarizes the take-away messages and then gives an outlook on what further research could look like.

2 Theoretical Background

To set the environment for this research and further discussion, some theoretical background knowledge is provided in the following chapter.

2.1 Debate about Land Cover Classification

To start out, a short discussion about land use and land cover is in order. In a multitude of remote sensing change detection studies, the terms 'land use' and 'land cover' are used interchangeably (Seto et al., 2002). The perception is that a certain 'land cover' corresponds to a certain 'land use', and therefore these words may be used as synonyms. An example for this would be shrub land. The land cover would be shrub land, as well as the land use. But there are instances where this direct connection does not exist and in these cases it is very important to distinguish between land cover and land use. An example for this would be the broader classification of agriculture. In this case, the land cover would technically be the crop type, but to summarize different crop types as well as the bare field used for farming crops, the land use 'agriculture' is used. Another example, especially relevant to this thesis, is the complexity of classifying urban features. Depending on the perception, this can refer to a particular land cover (e.g., concrete, steel and brick) or it can refer to a type of land utilization, and therefore land use (e.g., residential, commercial and suburban). Hence it is important to distinguish between cover and use as well as define what is incorporated in the classes. To summarize, the core difference between the two is that land cover only measures the physical attributes, conditions and characteristics of the earth's surface, while land use represents the utilization of the land cover (Seto et al., 2002). Since the main data source of this thesis is remotely sensed data, the focus will be on land cover, due to lack of further information to determine the utilization. A linkage of both is nonetheless possible with sufficient ancillary data and knowledge.

This leads to the discussion of land use classification schemes, often referred to as land use land cover (LULC) classification schemes. The standard CORINE Land Cover nomenclature is hierarchical, divided into three levels and includes a total of 44 classes (Manakos & Lavender, 2014). It is based on the CORINE land data base provided by the European Environmental Agency (EEA, 1994). One of the main issues with using this classification scheme is that many of the classes are dependent on the knowledge of land use. Hence the classification already represents an interpretation and is therefore not adaptable for this research. In addition to this, the classification is based on the land use land cover classification of Europe, which could comprise further problems by trying to adapt it to the classification of areas in Accra, Ghana, due to many differences in climate (e.g. vegetation) as well as urbanization processes.

Consequently, a classification scheme used for studies in the Global South should be considered. Kassawmar et. al. published an article on "Reducing landscape heterogeneity for improved land use and land cover (LULC) classification across the large and complex Ethiopian highlands" in 2016. There, they present a LULC classification approach that accounts for landscape heterogeneity. The classification scheme is divided into two levels and includes a total of 32 classes. On the first level they present the following nine umbrella classes: forest, woodland, shrub land/ bush land, cropland, agroforestry, grassland, wetland, barren land and settlement. In this classification, there are also classes, where the utilization has to be known to classify it accordingly. Nevertheless, this classification is much more adaptable to this research than the CORINE land cover nomenclature. In consideration of the study area, some of these classes are not present in the area of interest, but the classification in this thesis is nevertheless derived from the classification presented by Kassawmar et. al. (Kassawmar, Eckert, Hurni, Zeleke, & Hurni, 2016).

2.2 Synopsis of Land Use Cover Change Applications

Land use and land cover information is an important part of a variety of scientific activities and tasks, for example hydrological modeling, climate models, land use planning, as well as a key input to model ecosystem services (Manakos & Lavender, 2014; Gómez, White, & Wulder, 2016). The core of these analyses are space- and air-borne remote sensing techniques coupled with in situ observations and field information (Manakos & Lavender, 2014). In an temporal context land use cover change (LUCC) information, using multiple-year data, is just as valuable and has become an additional irreplaceable observation feature. "Qualitative changes in landscapes occur either as natural phenomena (wildfires, lightning strikes, storms, pests) or can be human induced (selective logging, agroforestry). Quantitative land-cover change is the wholesale categorical transformation of the land, and although it can occur as a natural phenomenon as caused by fires and storms, large-scale replacement of one land-cover type by another is usually induced by human activity (forest clearing, agricultural expansion, urban growth)" (Seto et al., 2002). In the past global land cover maps were generated from coarse spatial resolution (>100 m) data and resulted in low accuracy, especially in regions with heterogeneous land cover (Gómez et al., 2016). Nevertheless, since the open access to the USGS Landsat archive in 2008, Landsat data (TM, ETM+, and OLI) with a medium spatial resolution (10 - 100 m) became the standard for land cover classification and change detection (Gómez et al., 2016). Now, through new remote sensing technology such as satellites with more advanced sensors and drones, imagery with higher spatial (<10 m) and temporal resolution as well as additional spectral bands, are available. This leads to an interest in using this imagery for potentially more accurate analyses (Boyle et al., 2014). Johnathan Fisher et al. (2017) found out that higher-resolution imagery improves land use classification accuracy, however they emphasize the importance of the selection and usage of ground reference points in the analysis of the accuracy (Fisher, Acosta, Dennedy-Frank, Kroeger, & Boucher, 2017). In addition to this, temporal series approaches have been proven to be superior to single-date methods for a range of applications, including LUCC detection (Gómez et al., 2016; Broich et al., 2011; Franklin et al., 2015; Gómez, White, Wulder, & Alejandro, 2014).

There are different approaches to implement a land use classification. For this, multiple factors have to be considered: type of data, statistical distribution of classes, target accuracy, ease of use, scalability and interpretability of the classifier. However, it is important to establish a balance between acceptable accuracy and an optimal use of resources, as well as being aware that there are some trade offs between factors. Depending on the focus and method one can use single land cover classes (also referred to as two-class characterization) or the more common multiple-class characterization (also referred to as multi-class characterization) (Gómez et al., 2016). For the actual classification there are algorithms which cluster data by similarity of attributes without human intervention beforehand, such as an unsupervised classification. For these algorithms no knowledge of the land cover types has to be available. Clustering algorithms (e.g., k-means, ISODATA) aim to find subgroups within observations, such that objects in the same group (clusters) are more similar to each other than others 'outside' the group or cluster. Although clustering is an unsupervised machine learning technique, the found clusters can be used as features in a supervised machine learning model. This leads to the alternative of a supervised classification. For a supervised classification one uses an adequate number of good quality training samples. The selection of the training samples is crucial and usually a time consuming task, which is often done manually, although there are conditions for a semiautomatic selection. "Selecting and labeling samples is not error-free and potentially the cause of poor and biased classification performance" (Gómez et al., 2016). This is due to the fact that the supervised method requires the training data to completely represent the data, and therefore the classification problem, because the method is not capable of classifying something which is unknown to the training samples. Due to the increase of ancillary data, which improves the training data, a shift of the state of practice for land cover mapping from unsupervised techniques to supervised techniques has occurred in the last decade.

Further approaches can involve various classifiers used in parallel or in succession, which can be unsupervised as well as supervised. Between classifiers there is a distinguishment between parametric classifiers and non-parametric classifiers (Gómez et al., 2016). Examples for the parametric supervised classifiers are maximum likelihood, minimum distance and discriminant analysis, which are difficult to use with multi-temporal data of many spectral features and multimodal distributions (Glanz, Carvalho, Sulla-Menashe, & Friedl, 2014). Non-parametric classifiers such as k-Nearest Neighbor, decision trees (DT), neural networks and Support Vector Machines "impose boundaries of arbitrary geometries and provide higher flexibility at the expense of computationally intense iterative processes. In general, non-parametric classifiers that focus decision rules on class boundaries are proficient when the statistics and distribution of land cover types are unknown" (Gómez et al., 2016). A decision tree (DT) is an algorithm based on recursive binary partitions, where at each node certain attributes are checked, to lead to the next node. This method has its strengths in the ease of application (quick training, rapid performance) as well as interpretation. It it also able to handle data measured on different scales, having non-linear relationships and also missing data. A drawback of DTs is that it has been shown to perform less well than neural networks and Support Vector Machines relating to high dimensional data as well as that they are sensitive to noisy observations and over-fitting (Gómez et al., 2016). Random Forest (RF) is a variation of a DT, where the best matching tree out of a forest of trees (created by repetitive modification of the training data) leads to the classification (Belgiu & Drăgu, 2016). This leads to a higher accuracy than other DT and negates over-fitting. In exchange, the computational intensity is increased and the decision rules have a black box nature (Gómez et al., 2016). The Random Forest method is the chosen method that is used for the land cover classification in this thesis (see chapter 3.2). There is the possibility to combine the strengths of various algorithms into an ensemble classifier to increase accuracy, which can lead to an increase of computational complexity and a decrease in interpretability, such as Random Forest bagging and boosting (Gómez et al., 2016). Since this would exceed the extent of this research, these possibilities will not be further elaborated here.

When analyzing urban land cover information spatial resolution (i.e., smaller pixel size) is often considered more important than spectral resolution (i.e., more spectral bands or narrower intervals of wavelengths) (Myint, Gober, Brazel, Grossman-Clarke, & Weng, 2011). With better resolution more detailed features are visible, which can complicate urban features in relation to the spectral signature. This is caused by the density of many small objects, with various spectral signatures, in small areas; especially inside the urban setting. This leads to a potentially lower accuracy in urban image classification (Myint et al., 2011). Cowen et al. (1995) stated that a minimum of four spatial units (e.g., four pixels) must be inside an urban object area to be effectively identified, when using remotely sensed data. This means the spatial resolution of the used images has to be at least one-half the diameter of the smallest object of interest (Cowen et al., 1995). This practical approach does not completely go with the theoretical definition of the spatial resolution being the smallest linear separation between objects that can be separated in an image (Jensen, 2005). Nevertheless, even the practical approach can be difficult to fulfill, because the smallest object of interest will most likely not be perfectly located over four pixels, therefore a resolution much smaller than the object to identify is needed (Myint et al., 2011). As an alternative to the per-pixel approach of classification, there is also the object-based classification. This method separates spatially and spectrally similar pixels at different scale levels as segmented objects (Myint et al., 2011). Goal of this method is to effectively identify urban land cover classes, since it not only considers spectral information but also spatial information as well. It has been shown that the object-based classification can identify urban land cover classes with a higher accuracy than the traditional per-pixel approach (Liu & Xia, 2010; Myint et al., 2011). Nevertheless, one of the most significant potential limitation of the method is the determination of an appropriate segmentation scale and therefore on the quality of segmentation (Liu & Xia, 2010; Shackelford & Davis, 2003). Otherwise the classification could suffer from over- and under-segmentation, which creates objects that do not accurately represent real-world features (Möller, Lymburner, & Volk, 2007). Under-segmentation creates bigger objects then the objects are in reality and therefore they also cover mixed classes, while over-segmentation divides objects into smaller parts and should be merged to create a more realistic representation. This can reduce the accuracy of the classification (Hussain, Chen, Cheng, Wei, & Stanley, 2013). Due to the resolution and size of the object of interest the segmentation could also result into impractical segment sizes, as the added value from the pixel based approach could be minor. To remove the additional source of error, this thesis will focus on the traditional method of the per-pixel approach.

To detect land cover change one needs to analyze a time series. In this regard, there are two fundamental approaches: Firstly, independent land cover maps can be generated for each time step, which are then used to determine change between each time step. Secondly, a base map (representing reference date conditions for a single year) can be generated, which then can be up- and backdated with change information obtained from a spectral time series. The latter is referred to as the change updating approach and is especially interesting for monitoring purposes. (Gómez et al., 2016). In terms of detection logic there are two major types. Firstly the hard change detection and secondly the fuzzy[1] change detection. Due to the increase in complexity, the fuzzy pixel method is not used (Jensen, 2005). The more common method seems to be the comparison of multi-temporal hard land cover classifications. This results into hard change detection maps, where the land cover change is shown in change from one category to another. The hard change detection is dependent on the type of classification in regards to pixel-based or object-based, since it is a post-classification (also called delta classification) comparison. One advantage of this approach is that the images are classified separately, therefore they don't have to be radiometric corrected (calibrated) as much as with other change detection approaches (Coppin, Jonckheere, Nackaerts, Muys, & Lambin, 2004). Alternatively the change detection is based on fuzzy land cover classification data, where also more discrete changes can be detected. In general the accuracy of delta classifications depend heavily on the quality of the initial classifications (Coppin et al., 2004). Further change detection techniques are, but are not limited to, image differencing, image regression, image ratioing, vegetation index differencing, principal component analysis and change vector analysis (Seto et al., 2002).

2.3 Conception of Patterns and Comparative Methodology

Like other concepts mentioned beforehand, the term 'pattern' can also mean something different depending on the point of view. In a dictionary one would find a definition similar to: "A pattern is a regular and intelligible form or sequence discernible in the way in which something happens or is done" (Google dictionary, 2018). The detection of patterns in scientific research can happen on different data foundations. This can include quantitative data such as air-borne and population data, as well as qualitative data such as survey and interview data. In relation to land cover change patterns, studies are often based on quantitative data and spatial analysis as shown in these examples: "Spatial Pattern of Land Use Change and Its Driving Force in Jiangsu Province" (Du, Jin, Yang, Yang, & Zhou, 2014), "Urban Development in West Africa - Monitoring and Intensity Analysis of Slum Growth in Lagos: Linking Pattern and Process" (Badmos, Rienow, Callo-Concha, Greve, & Jürgens, 2018) and "Pattern of Population Growth in Peri-Urban Accra, Ghana" (Doan & Oduro, 2012).

The latter mentioned study by Doan and Oduro (2012) presents four hypothesis on processes of urbanization. While basing their research on population census data from 1970, 1984 and 2002, spatial modeling and regression analysis, they prove that urban expansion at the edge of the city Accra is not amorphous, but expands according to recognizable patterns. For this, they formulate four hypotheses based on qualitative analyzes of literature. They combine descriptions

[1]Fuzzy classification techniques allow pixels to have memberships in more than one class and thus represent the imprecise nature of data (Shackelford & Davis, 2003).

of urbanization phenomena in literature with own observations and formulate hypotheses to explain 'peri-urban'[2] growth. The *spreading pancake* is the first hypothesis. In this assumption the city spreads in a series of concentric rings about the central city. With increasing distance from the center of the city the rate of population density declines. Thus the idea behind this hypothesis is the proximity to the main city. *Development node* is the name of the second hypothesis, which states that localities close to a cluster of global investment are likely to experience a higher urbanization rate. Therefore this focuses on the proximity of economy. As the next hypothesis, they present *village magnet*, where localities in close proximity to existing villages are predicted to urbanize more quickly. This implies the importance of already existing infrastructure of some sort. This existing infrastructure is not restricted to water or electricity supply, but can also include already existing communities. At last, they introduce the *ribbon* hypothesis. With this, they predict higher urbanization rates for communities located along highways. (Doan & Oduro, 2012). This hypothesis as well could indicate the importance to the central city, since highways and bigger street are of most use to commuters. All four of these hypothesis try to explain a qualitative phenomenon, but are measured in a quantitative way. These measurements result in patterns, which can be detected. Since this research is based on Census data, which is tied to district boundaries, these hypothesis are hard to translate into today, due to districts boundaries changing over time (see chapter 2.4) and therefore a comparison is difficult. This is why it will be tested if these hypotheses can be found based on satellite imagery and on a smaller scale.

Seeing that data is difficult to compare, in the following general conditions for comparison are described. Comparisons are one of the most common and at the same time one of the least reflected procedures in geography (Vogelpohl, 2013). They do not serve primary as illustrations, but on the contrary they should be an approach to lay down similarities and differences between cases to help identify spatial processes and asses their relevance. Essentially all scientific analysis contain a comparative element, if not through several case studies, then along comparative dimensions. In the following table (2.1) four different comparison dimensions are defined according to Anna Vogelpohl (2013).

These dimensions are not mutually exclusive, but are closely related and partly mutually constitutive. The focus, however, depends on the question. In a critical reflection of comparative works with the title 'Comparing and Miscomparing', Giovanni Sartori (1991) names three questions that all comparative studies must answer:

1. *Why* Compare?

2. *What* is Comparable?

3. and *How*?

While these questions seem self-evident at first glance, many studies do not raise these questions and therefore come to wrong or poorly substantiated results or fail to exhaust the qualities of comparisons (Sartori, 1991). Satori claims that basically no knowledge of a case is possible without 'controlling' it with (another) and learning from the other experiences. To answer the

[2] The term 'peri-urban' is used since the referenced literature refers to the urban expansion of Accra as such, but it is not used to state that the urban expansion of Accra is considered peri-urban opposed to suburban, exurban, rural-urban fringe or etc..

Table 2.1: Comparison dimensions (Vogelpohl, 2013)

Spatial	Comparisons between spaces allow the simultaneous recognition of spatial specifics and generalizable relationships that produce space. Rooms of the same scale level can be compared or different scale levels can be compared.
Temporal	Snapshots at different times reveal changes in individual social structures, functions or forms. The time dimension can be compared either over long historical periods or over the course of annual or even times of the day. While historically-based comparisons make fundamental transformations or continuations understandable, comparisons of shorter time periods allow the interaction of different simultaneous processes.
Socially-lived	Social conditions are produced and perceived differently by different individuals, groups and institutions in different ways. Social differences along e.g. status, gender, lifestyle lead to other levels of concern and assessments.
Conceptually-normative	Situations and processes, often implied, are compared to habitual or desired situations and processes. All descriptions, and in particular valuations, refer to a reference that is to be understood as "normal state," "average," or "ideal state." This problem becomes very clear in the development of general principles, models and scenarios that always convey norms.

first question of Sartori (1991) Vogelpohl (2013) introduces four types of comparison which, same as the dimensions mentioned above, are not mutually exclusive. This typing may help to establish and justify the line of the comparison, and thus the choice of case studies and analysis aspects.

Table 2.2: Types of comparison (Vogelpohl, 2013)

Individualizing	The comparison dimensions are designed in a contrasting manner, so that the respective peculiarities of the cases are highlighted.
Universalizing	The comparison shows that specific phenomena always work according to the same schemata or mechanisms and therefore permit structural conclusions.
Variations finding	The similarities between the cases vary in nature and intensity. This type of comparison illustrates gradual gradations of a phenomenon.
Amalgamating	The juxtaposition of cases in different places shows that both belong to a common system of a common structure, albeit in different ways.

Although this framework is designed for qualitative comparisons, it will be used in this thesis. The line between qualitative and quantitative paradigms can be defined in multiple ways, such as in the way in which each tradition treats data (Brannen, 1992). As "the qualitative researcher is said to look through a wide lens, searching for patterns of inter-relationships between a previously unspecified set of concepts, (...) the quantitative researcher looks through a narrow lens at a specified set of variables" (Brannen, 1992). The differences which researchers feel exist between qualitative and quantitative approaches have extensive effects on the focus and conduct of research projects and especially the choice of method. Due to the interdisciplinary approach of this thesis, these boundaries will be ignored in this research and this framework will be used to compare the resulting data of this research (Brannen, 1992).

2.4 Accra, the Densu Delta and Surrounding Areas

Since the middle of the twentieth century Ghana has encountered a very rapid urbanization rate (Yankson & Bertrand, 2012) and in the past 20 years Ghana experienced expeditious urbanization, with a higher urbanization rate then the global average and it even surmounted the West African average (The World Bank Group, 2015). However, modern urbanization in Ghana is focused mostly on Accra-Tema and two other urban cores (Yankson & Bertrand, 2012). Therefore, Ghana's coastal capital city Accra is one of largest cities in West Africa, and is projected to be growing at a rate of 4.59% in the current decade (UN Habitat, 2014).

There are many factors which influence the urbanization of African cities, these range from current and historical governmental planning practices over traditional land ownership systems, private development interests to direct foreign investment and migration (Frick-Trzebitzky, Baghel, & Bruns, 2017). Nevertheless the high population rate is, as in many other African countries, the result of a combination of firstly high rates of natural national population increase and secondly a net in-migration to the urban areas. In addition to this, the two processes reinforce each other, although the relative importance has varied over the past (Yankson & Bertrand, 2012). Concomitant with the growing population is the physical expansion of cities which lead to changes in official boundaries, trying to keep up with the expansion. After the independence of Ghana in 1957 the Greater Accra Metropolitan Area (GAMA) consisted of the Accra metropolitan assembly (AMA), Tema municipal assembly (TMA) and the Ga district assembly (GDA) (Grant & Yankson, 2003). The increase in population over the following 40 years is shown in table 2.3.

Table 2.3: Population of GAMA by district from 1960 - 2000 (Yankson & Bertrand, 2012)

District	1960	1970	1984	2000
Accra	388,396	636,667	969,195	1,658,937
Tema	27,127	102,431	190,917	506,400
Ga	33,907	66,336	132,786	550,468
Total GAMA	449,430	805,434	1,922,898	2,715,805

Between 2000 and 2010, due to the growth of population, the district boundaries were adjusted. All boundaries were expanded or shifted somewhat. Due to a lack of information available it is hard to determine the exact changes. Nevertheless, roughly speaking GDA was divided into GA South, GA West and GA East, while TMA was divided into Tema and Adenta and AMA was divided into AMA and Ledzokuku/Krowor (LEKMA). Furthermore the districts Dangme

West and Dangme East were added (Yankson & Bertrand, 2012; Ghana Statistical Service, 2013, 2014a, 2014b). The newest population data per district is presented in table 2.4.

Table 2.4: Population of GAMA by district from 2010 (Ghana Statistical Service, 2013)

District	2010
Ga South Municipal	485,643
Ga West Municipal	262,742
Ga East Municipal	259,668
Accra Metropolitan Area	1,848,614
Adenta Municipal	78,215
Ledzokuku/Krowor Municipal	227,932
Ashaiman Municipal	190,972
Tema Municipal	402,637
Dangme West	122,836
Dangme East	130,795
Total GAMA	4,010,054

The districts of most interest to this research are AMA and Ga South, since the border between these two districts runs through the study area (see fig. 2.2). As visible in the following table 2.5, the growth rates[3] of both districts differentiate quite a bit. While the growth rate in Ga South increases continuously throughout 1960 to 2000, the growth rate in AMA fluctuates, but remains positive and under 1. Unfortunately the available data between 2000 and 2010 is not comparable, due to differences in district boundaries but also differences in survey methods, therefore the growth rate between those time frames could not be calculated. The overall growth rate of GAMA over time varies significantly in literature and is therefore not presented.

Table 2.5: Population growth rate in Ga South and AMA from 1960 to 2000

District	1960-1970	1970-1984	1984-2000
Ga South	0.95	1.00	3.15
AMA	0.64	0.52	0.71

Moving towards the general conditions around the capital city of Ghana, Accra is bounded by the Gulf of Guinea in the south (Grant & Yankson, 2003), while the Greater Accra Region lies within a dry equatorial climatic region, which is referred to as the central and southeastern coastal plains. The coastal lands of Ghana have two seasons: the dry season and the rainy season. The main rainy season occurs from April to June, while the second, minor rainy season is September through October (see figure 2.1). The highest precipitation usually happens in June (Finlayson, Gordon, Ntiamoa-Baidu, Tumbulto, & Storrs, 2000).

[3]Based on the population data of GAMA from 2010 in table 2.3

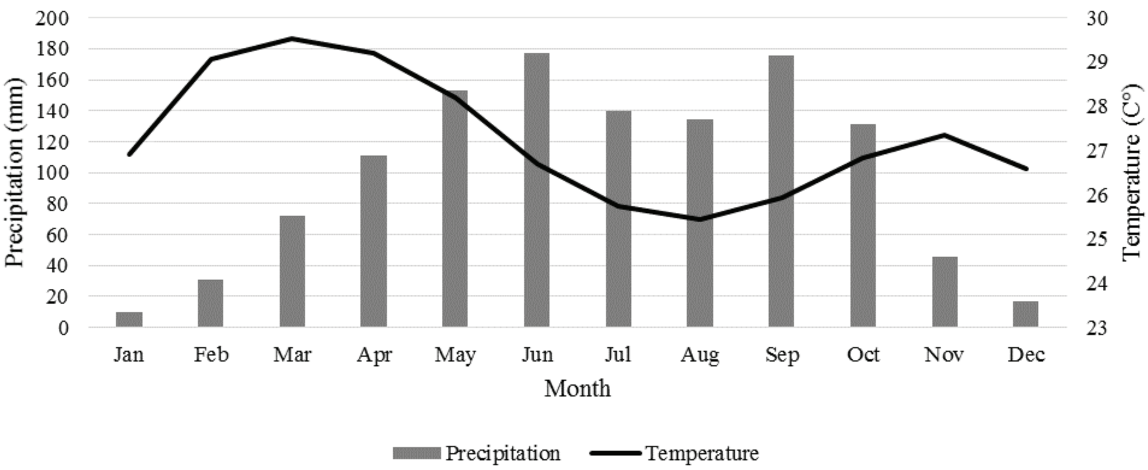

Figure 2.1: Average monthly temperature and rainfall for Ghana from 1901-2015 (The World Bank Group, 2018)

The focus of this research is the Densu delta wetland and its surrounding areas (see fig. 2.2). The delta wetland occupies approximately 60 square kilometer west of downtown Accra. The main river which drains into the wetland is the Densu river. Since the river is controlled by the Weija dam, which is located circa 11 km stream upwards, during dry season the wetland has no direct connection to the sea, but during rainy season the Weija dam lets more water pass, which often leads to flooding and therefore to discharge into the Gulf of Guinea (Kondra, 2016). Right next to the delta and inside the wetlands, using an area of roughly 11 km^2, the Panbros Salt Company harvests salt through solar evaporation (Kondra, 2016; Affam & Asamoah, 2011). Additionally, the Densu delta area is one of Ghanas Ramsar sites. The Ramsar convention entered into force in Ghana on the 22nd June of 1988. Currently, Ghana has six sites designated as wetlands of International Importance (The Ramsar Convention Secretariat, 2014). "The Densu delta is managed according to the wise-use principles of Ramsar convention under the authority of the Wildlife division of the forestry Commission of Ghana, which explicitly does not exclude people and resource use" (Tyroller, 2016). This is the reason why the Panbros Salt Company can pursue their business and also why there are settlements within the wetland, around the delta, and even a large informal[4] settlement inside the delta itself.

[4]In this thesis 'informal' is not meant in the context of approval from the government, but rather an area which is self built.

Figure 2.2: The Densu delta and surrounding areas (Tyroller, 2016; European Space Imaging, 2017)

3 | Method

In the following chapter the data and it's complete processing is described and explained. Firstly the used data is introduced and the procedure of pre-processing is shown. Following this, the random forest classification of the satellite images is elucidated. Lastly the conduction of a land cover change and pattern detection is clarified.

3.1 Data and Pre-processing of Imagery

The data used in this research was obtained by the European Space Imaging in early 2018 (European Space Imaging, 2017). The goal for acquiring data was to find the most recent, mostly cloud free image, with a relatively high resolution and at least one image dating back as far as possible, to detect land cover change over a long period of time. Since the smallest object of interest in this study are urban objects, such as kiosks with a size of approximately 15 m^2 the diameter of the resolution should be at least 5.5 m. This research finalized in images out of two time ranges. Firstly an image out of 2017 (recording time: 23.03.2017; see fig. A.2) and secondly a mosaic from different images out of 2008 to 2010 (recording time: 15.12.2008, 16.05.2009 and 12.01.2010; see fig. A.1). The latter is compiled out of three years, since the region could not be covered nearly cloud free by imagery out of a single year. Unfortunately it was not possible to obtain an image dating even further back with the same quality, due to the high cloud coverage of the research area. Nevertheless, the resolution of both images is 1.5 m, which results in a diameter of 2.1m, which is satisfyingly smaller than the goal of 5.5 m. Since the research is in cooperation with the WaterPower Project, whose research area is the Greater Accra Metropolitan Area (GAMA), this was also the extent of the satellite data search. The images were taken by two commercial earth observation (EO) satellites owned by DigitalGlobe, which are named QuickBird-2 and WorldView-2 (Satellite Imaging Corporation, 2017b, 2017a). Both satellites capture the earths surface using panchromatic and multispectral bands (see tables A.1 and A.2 in the appendix for bands and their spectral wavelengths). For this research the four multi-spectral bands both satellites have in common (blue, red, green and Near-infrared (NIR)) will be used. Further ancillary data such as a digital elevation model (DEM) and light pollution maps were researched, but there is no available data with the needed resolution. The image section used in this analysis is based on the images available for the area around the Densu delta. As one can see in image A.1 in the appendix, the mosaic image from 2008-2010 has a notch in the top left corner, therefore the subset was set, so that both images entail the same extent (see fig. A.2).

Before the imagery can be used for classification and analysis, the images have to be corrected to eliminate unnecessary errors. The first step is to geometrically correct the images, so that the 2008, 2009 and 2010 images can be compiled as a Mosaic in the next step. For the geometric correction the image from 2010 was used to geometrically correct the images from 2008 and 2009, as well as 2017 through areas of overlap. The geometric correction in the temporal context is especially important to prevent false change detection based on wrong pixel locations. This step can lead to a slight alteration of the pixel sizes, which is important to consider later on when calculating the extent of areas. During the second step, mosaicking, the images are color corrected through a histogram matching based on image overlap areas. "Mosaicking is the process of combining multiple images into a single seamless composite image" (Jensen, 2005). Histogram matching means that the histogram from the base image (2010), is extracted and then applied to the other images (2008 and 2009) using a histogram-matching algorithm. This leads to the images having approximately the same gray-scale characteristics (Jensen, 2005). Since only the two time frames are compared and the images are not prepared to compare with other satellite images, the calculation of the 'top of atmosphere radiance' is not necessary and the histogram matching is sufficient. Furthermore, areas which complicate the classification process (through spectral signatures which are similar to other spectral signatures) but bring no added value to the analysis and later interpretation were masked out (i.e., clouds and the salt ponds). An attempt was made to keep the salt ponds included, but the classification had a hard time dealing with the signatures, so the algorithm would have had to be trained to recognize it as salt ponds. The added value was then considered not worth the extra effort. To help the separation of vegetation from other classes the Normalized Difference Vegetation Index (NDVI) was calculated, stretched to 8-bit and added as a fifth layer to the four band layer stack. The NDVI is a normalized ratio of the NIR and red bands (Huete et al., 2002). The analysis of the two districts which adjoin in the study area is supported by using a shapefile from the Town and Country Planning Department showing the boundaries from 2016, which are still up to date for 2017 (Akubia, 2018). Compared to the borders presented in the Census Data from 2010 there has been no change in our study area (Ghana Statistical Service, 2013) and therefore it can be used in both time frames. In addition to the pre-processing, a pre-analysis was conducted, where several classification methods were tested on both images to find out how well they performed with the given data and its difficulties. This resulted in the usage of the classification method Random Forest. All pre-processing computations, pre-analysis and further analysis are conducted using the programs ERDAS Imagine (from Hexagon AB) and ArcMap (from Esri's ArcGIS).

3.2 Random Forest Classification

Due to the accuracy of the random forest[1] (RF) classification, the speed of processing, capacity to handle both high dimensional and multicolinear data, as well as its insensitivity to overfitting, this classifier has received increased attention over the last two decades. Especially the accuracy, the speed of processing and the capacity to handle multicolinear data are compelling for this thesis. "The RF classifier is an ensemble classifier that produces multiple decision trees, using

[1]Random forest was developed by Breiman and is considered a machine learning method (Breiman, 2001).

a random selected subset of training samples and variables" (Belgiu & Drăgu, 2016). In other words, it is a combination of tree classifiers, where each classifier is generated using random variables sampled independently from the input variables (Pal, 2005). Through the black box nature of RF, the decision rules are obfuscated (Gómez et al., 2016). In the end, the classification is decided through majority voting (see fig. 3.1).

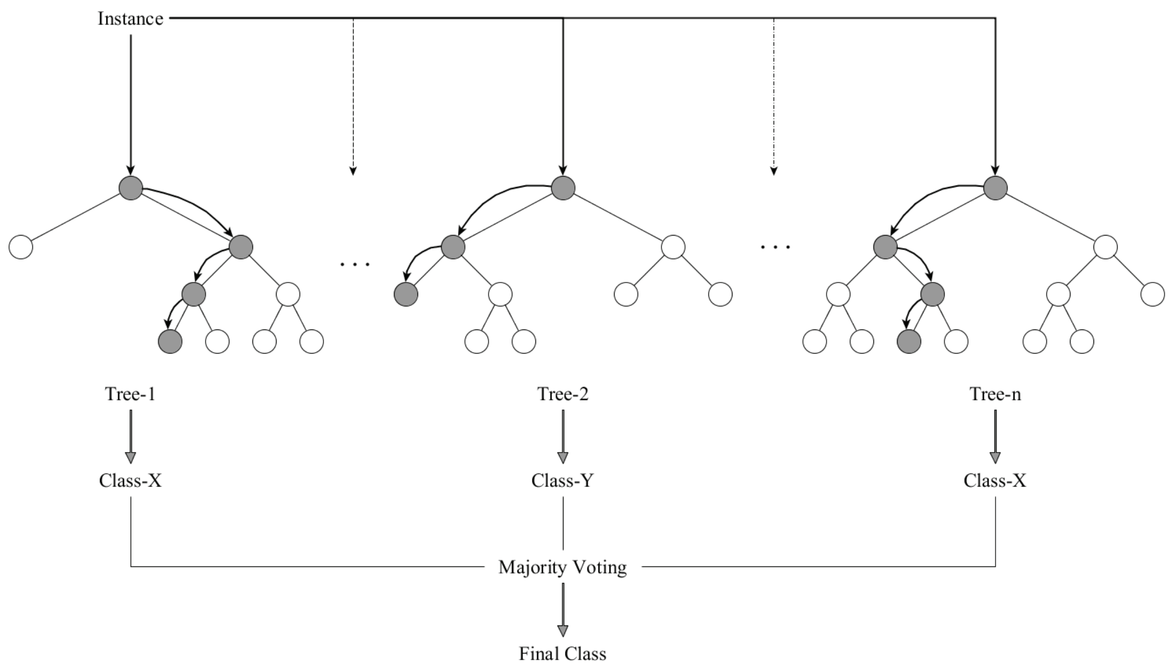

Figure 3.1: Example Random Forest Classification Schematic: While training the RF algorithm a RF network is constructed. The network includes a random number of DT (in this example three), which consist of a random number of nodes from random variables (in this image grey circles). The height (number of nodes between starting node and leaf) of the trees is also random. With the leaf of the chosen branch the class of the pixel for each DT is decided. After this the final class of the instance is determined through majority voting, considering all DTs of this instance. In this example the final class would be Class-X. This is done for every pixel in an image using the same RF network.

To perform a random forest classification, a set of training data has to be prepared (Hexagon AB, 2017). In preparation to create the training data, a classification scheme has to be set. For this several LULC classification schemes are available. The following classification scheme is inspired by Kassawmar et al. (2016) with two levels of classes. Since one-level classifications are often not sufficient in representing the complexity of land cover pattern, the second level of classifier is used to capture image-related peculiarities, such as water reflection (Kassawmar et al., 2016). One peculiarity for the classification of the image from 2008 - 2010 was that the image from 2009 was taken during the raining season, while the images from 2008 and 2010 were taken during the dry season. The difference of the vegetation spectral signature was considered in this instance and therefore separate classes were created for the especially saturated vegetation. As training data, over 4000 training points (point clouds) were manually created and classified into different classes as shown in table 3.1 (Level II) for each time frame. The level I classes are the classes to be used for change and pattern detection. Although the classes 'vegetation' and 'bare land' could stay in more differentiated classes, the focus is on urban land cover, thus more differentiation would not bring added value for the study. A more differentiated classification of the level I class 'urban' would have been useful in this analysis. Unfortunately the spatial signatures of different urban classes such as buildings with and without roofs, etc. (except by color) were not sufficiently distinguishable, therefore urban is classified as one class on level I.

Table 3.1: Nested hierarchy classification scheme of land-cover, differentiated by level of detail.

Level I	Code	Level II	Code
Bare Land	1	Bare Land	6
		Muddy Soil	19
		Sand	5
Vegetation	2	Grass	1
		Saturated Grass	3
		Shrubs	2
		Saturated Shrubs	4
Urban	3	White buildings	7
		Colorful buildings	8
Tarmac	4	Tarmac	9
Water	5	Turbid Water	11
		Seaweed Water	12
		Reflection	21
		Clear Water	10
Not Classified	0	Black	20

The next step is running a spatial model (in the program ERDAS Imagine) to compute raster statistics for each time frame, in this case the value of each pixel per band, per training point. The values per band will be the variables, which are used in the following RF classification. Before the images can be classified, the RF algorithm has to be trained with the prepared training data. This is computed with another spatial model, where the variables (values per band) and their assigned classification name (Level II) are used to train the machine intellect (also known as Random Forest network). It is important to note that whatever information was used for training, also has to be available for the data which is to be classified. During the training the algorithm constructs a random forest network which best describes the relationship between the classes and the variable information associated with each class. Regarding this, the machine intellect output is then used to classify the raster image from each time frame, by using the RF network to classify each pixel based on its band values. This produced an image where each pixel is assigned the most probable class based on the RF algorithm (Hexagon AB, 2017). After the RF classification the level II classes are summarized and reclassified into the regarding level I classes (see table 3.1).

This whole process is repeated many times while adjusting the training data each time, to compute a better classified image.

3.3 Accuracy Assessment

Although the accuracy of classification methods are improving, any map based on remotely sensed data contains some error and is potentially subject to bias. An accuracy assessment can identify the errors of classifications. To assess the accuracy of a classification, reference data from different sources, such as ground truth data, aerial photography or other satellite imagery can be used. The data should preferably have an equal or finer level of detail than the classified data. The temporal aspect of the reference data should also be considered (Olofsson et al., 2014). The ideal would be if the date from the reference data is not far apart from the classification data, since changes (vegetation change during seasons, etc.) occurring in the gap time lead to discrepancies. Nevertheless this approach does have its limitations when there is a lack of data to choose from. For this thesis, there is no ground truth data or different satellite imagery with adequate resolution available. Therefore, the data used for the classification is also used as reference data. To reflect the reference data, similar to the training data, sample data is created assigned to the different classes (Level I). During the creation of the sampling data, a stratified random sample design was followed. As Olofsson et al. (2014) states, "stratified random sampling affords the option to increase the sample size in classes that occupy a small proportion of area to reduce the standard errors of the class-specific accuracy estimates for these rare classes. Thus this design addresses the key objective of estimating class-specific accuracy." For this research the sample size for each time frame was set to approximately 1000. These sample points were classified manually and if a point was not identifiable, they were discarded. This is important to keep in mind, since the accuracy of the classification is dependent on the analyst recognizing the land cover as the according class.

The analysis of the accuracy assessment starts with the formation of an error matrix (also know as confusion matrix), where the sample sites with class labels from the classification and reference data are cross tabulated against each other. While the main diagonal of the error matrix represents the correctly classified sample sites, the off-diagonal show the wrongly classified sample sites (omission and commission error). The values (p_{ij}) inside the matrix are proportioned to the total sample data site count. Whereas the rows of the matrix represent the classification classes (class i) and the columns represent the classes from the reference data (class j), the amount of classes is represented by q.

One very common accuracy parameter is the overall accuracy (O) which shows the fraction of correctly classified sample data in relation to the total number of validation points (n).

$$O = \frac{\sum_{j=1}^{q} p_{jj}}{n} \tag{3.1}$$

By calculating the user's accuracy (U_i) of class i, the probability of correct prediction is shown, therefore it represents how reliable the classification is.

$$U_i = \frac{p_{ii}}{p_{i*}} \tag{3.2}$$

Complementary, the error of commission of class i is calculates as 1 - U_i. The producer's accuracy (P_j) on the other hand shows the accuracy of the class j and therefore the accuracy of the classification.

$$P_j = \frac{p_{jj}}{p_{*j}} \tag{3.3}$$

It's complementary measure, error of omission of class j, is calculated as 1 - P_j. The kappa coefficient (κ), also known as Cohen's kappa, is a widely used, yet controversially discussed coefficient, which accommodates for the effects of chance agreement. "The problems associated with kappa include but are not limited to: 1) the correction for hypothetical chance agreement produces a measure that is not descriptive of the accuracy a user of the map would encounter (kappa would underestimate the probability that a randomly selected pixel is correctly classified); 2) the correction for chance agreement used in the common formulation of kappa is based on an assumption of random chance that is not reasonable because it uses the map marginal proportions of area in the definition of chance agreement and these proportions are clearly not simply random; and 3) kappa is highly correlated with overall accuracy so reporting kappa is redundant with overall accuracy" (Olofsson et al., 2014). Nevertheless, it is one of the most used coefficients to compare accuracies, which is why it is used in this research. Kappa is calculated as follows:

$$\kappa = \frac{n \sum_{i=l}^{q} p_{ii} - \sum_{i=l}^{q} (p_{i*} * p_{*j})}{n^2 - \sum_{i=l}^{q} (p_{i*} * p_{*j})} \tag{3.4}$$

Doing so, it takes into regard the number of correctly assigned pixels as well as the chance agreement, which is indicated by the row and column totals (Foody, 2002; Jensen, 2005; Olofsson et al., 2014).

3.4 Land Cover Extents and Change

Before the extents and change of land cover can be calculated, the three questions asked by Sartori (1991) should be addressed. The first question is '*Why* compare?'. For the analysis of the land cover extent, as well as the land cover change, the answer to this question is to find variations in urban growth (see table 2.2). While the comparative aspects might be finding patterns through analyzing variations, the analysis could lead to key aspects of different nature (Brannen, 1992), such as universalizing or amalgamating aspects. The second and third question are '*What* is Comparable? and *How*?'. The analysis of the status of urban extent for each time period is compared in a spatial dimension (see table 2.1), where the time frame is fixed. As for the analysis of change, the comparison is on a temporal dimension (see table 2.1), where the spatial extent is fixed. Both analyzes are compared using the same set of variables, extracted in the same way, as will be explained in the following.

In order to calculate the areas of each land cover, the pixel counts of each class (Level II) were summed up and then multiplied by the pixel size/ area. Since the sizes were altered during the geometrical correction, it is important to use the correct pixel size, otherwise the extent of land cover areas will be false. The pixel area of the image in 2008-2010 was alerted to the value of 2.35392766525225 m^2 and the pixels in 2017 were changed to 2.25091059211225 m^2. As a reference, without the geometrical correction the pixel sizes would have ben 2.25 m^2. Using a tool in ArcMap the class areas for each district were tabulated, from which the data could be extracted for further conversions. To further evaluate and compare different areas of the image, especially the districts, a grid was created. For this, square boxes with a side length of 1 km were generated through a 'Create Fishnet' function in ArcMap. Then the pixel counts of each class were extracted per box that intersected with the given district polygons. This of course leads to the boxes not including the same land extent, since areas are lost to cloud coverage, salt ponds, the ocean and the boundaries to other districts. To compare the land coverage anyhow, the values are converted to ratios. Since 'Bare Land', 'Vegetation' and 'Urban' are the dominant land cover classes, further analysis will focus on these three classes. An ideal way to display the proportions of three variables is a Ternary plot/ diagram (also known as Tri-plot). This is a barycentric plot based on three variables which sum up to a constant and is often used in earth sciences to show compositions. In view of using ratios for the three variables anyway, the constant in the Ternary diagram is 100%, which the ratios of the three variables add up to. This approach disregards the land cover classes 'Tarmac' and 'Water'. This was done due to water being mostly stationary, therefore it brings no added value to this research. Tarmac is disregarded due to the results of the accuracy assessment (see chapter 4.1) and due to its marginal total extent.

In order to detect land cover change, a post-classification change detection was conducted. For this, a matrix union of both images from 2008-2010 and 2017 was executed. In this matrix the amount of pixels which changed from one class to any other is visible, as well as the amount of pixels which stayed the same class. From the pixel counts the area of change can then be calculated. Since the pixel sizes were altered during the geometrical correction the area of each pixel is calculated through averaging the pixels size of both time frames. This leads to a pixel size of 2.30241912868225 m^2. Unfortunately this reduces the accuracy of the change detection, however the consequences of this will show in the result.

Furthermore, the overall change in square-kilometer can be easily calculated by subtracting the extent of each class in 2008-2010 ($A_{2008-2010}$) from the extent of the respective class in 2017 (A_{2017}). The relative growth rate can be calculated as follows:

$$Growth\ rate = \frac{(A_{2017} - A_{2008-2010})}{A_{2008-2010}} \tag{3.5}$$

3.5 Pattern Detection

In this analysis approach four areas are considered, each focusing on an area in context of the four hypothesis presented by Doan and Oduro (2012) (see chapter 2.3). For this the four areas will be analyzed using a Ternary plot. Doing this over the time period will show how the composition changes over the course of almost a decade. To set the areas of interest, certain criteria have to be fulfilled. Firstly the area has to be fully covered during both time frames, so no area near to cloud coverage can be used for this comparison. AMA is considered to belong to the city center and based on the results of the land cover change analysis, AMA did not change much over time. Therefore AMA is not well suited to prove the hypothesis and subsequently all sample areas are located in Ga South. Lastly, all areas of interest (AOI) have the same extent of 2 km^2 and are circular (see fig. 3.2). The first hypothesis states that the city grows in concentric circles, therefore an area (h1) which is located in the north of the study area and away from bigger roads and already existing villages was chosen. The second hypothesis predicts growth near global investment, therefore an area (h2) right next to the West Hill Mall was chosen. In foresight of the forth hypothesis this location is unfortunately next to Winneba Rd., but since global investments and larger road will always correlate it is impossible to detach both of them. For the third hypothesis, predicting growth near already existing settlements, an area (h3) just north of Tsokomey (Bortianor) was selected. The area (h4) considering the forth hypothesis - growth along highways - is located just west of the Densu river and south of Winneba Rd. From these areas the amount of pixels per class were extracted and the ratios of the classes 'Urban', 'Vegetation' and 'Bare Land' were plotted in a Ternary plot.

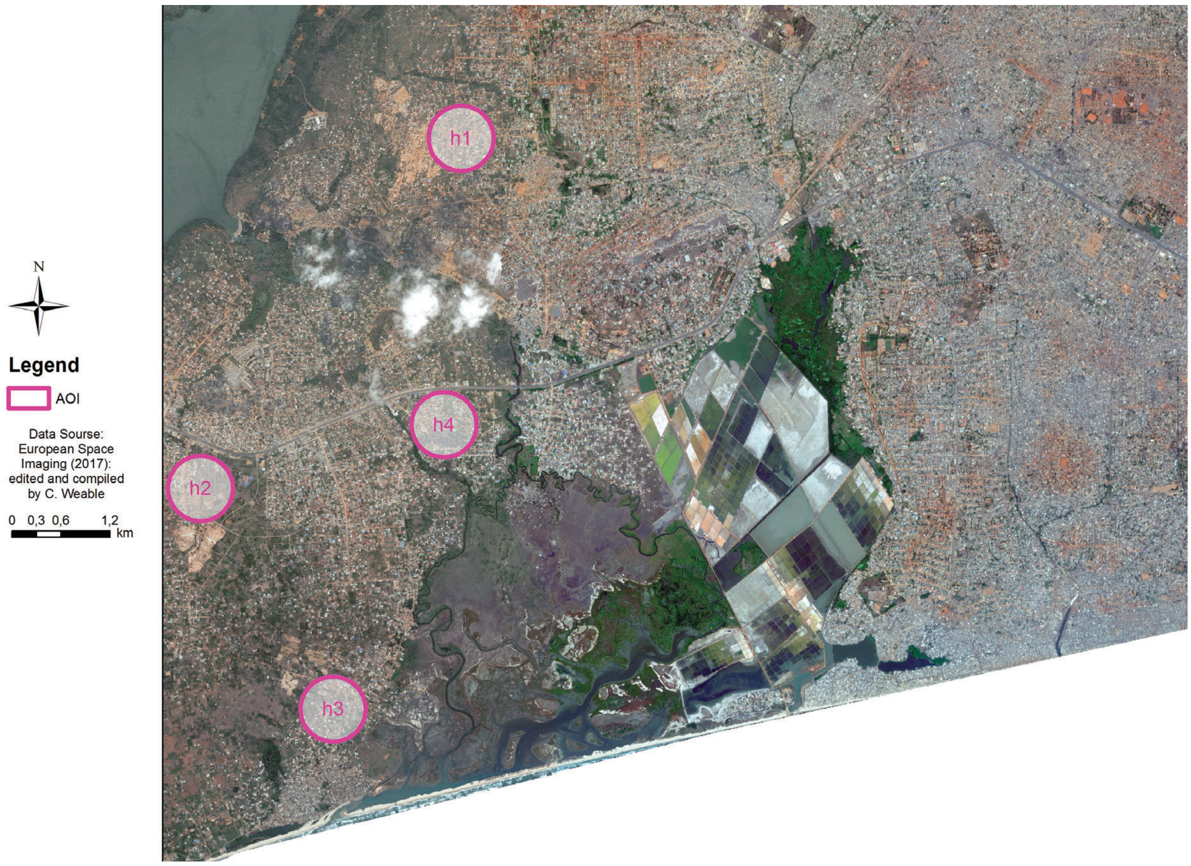

Figure 3.2: Locations of each area, which are used for the analysis of the four hypotheses presented by Doan and Oduro (2012)

4 Results & Discussion

4.1 Accuracy of Classification

As mentioned above, the results of the accuracy assessment are essential to interpret the outcome of a classification, since it reveals errors. The following tables 4.1 and 4.2 show the results of the accuracy assessments.

Table 4.1: Classification of 2008-2010: Error Matrix (values in proportion to the total amount of sample points) and Accuracy Parameters; (1) - Bare Land, (2) - Vegetation, (3) - Urban, (4) - Tarmac, (5) - Water, Com U_i - Error of Commission, Om P_j - Error of Omission.

		Reference							
		(1)	(2)	(3)	(4)	(5)	Total	U_i	Com U_i
Map	(1)	0.387	0.008	0.062	0.005	0.000	0.462	0.838	0.162
	(2)	0.002	0.230	0.000	0.000	0.000	0.232	0.990	0.010
	(3)	0.032	0.003	0.170	0.003	0.002	0.209	0.815	0.185
	(4)	0.003	0.000	0.001	0.009	0.009	0.022	0.412	0.588
	(5)	0.000	0.003	0.003	0.001	0.068	0.075	0.906	0.094
	Total	0.424	0.244	0.237	0.017	0.079	1		
	P_j	0.914	0.942	0.719	0.526	0.863		O	0.864
	Om P_j	0.086	0.058	0.281	0.475	0.136		Kappa	0.820

The classification of the image from **2008-2010** has an overall accuracy of 0.864, this means 86.4% of the reference data was classified correctly in the map. The kappa coefficient of this classification is 0.820. Kappa indicates how well the classification performed compared to a random classification[1], where 0 indicates that the classification did not perform better than a random classification and a value close to one indicates a perfect agreement. In this case, the classification is significantly better than a classification by mere chance. However, to find out where misclassifications occurred, an investigation of the producer's and user's accuracy can help.

As mentioned in the methods chapter, the producer's accuracy shows how often the real land cover is correctly shown in the classification map. In other words, the accuracy shows how well the map was *produced*. Three out of the five classes have a producers accuracy above 80%. The class 'Tarmac' shows the lowest accuracy with 52.6% and an omission error of 47.5%. This means that

[1] A random classification in this instance means a random assignment of values to the image pixels.

52.6% of pixels which represent tarmac were correctly assigned and 47.5% of these pixels were wrongly assigned to different classes, especially 'Urban' and 'Water' (compare table 4.1). There are several reasons for this. The confusion between 'Tarmac' and 'Urban' is mostly due to shade cast by buildings or clouds, which leads to an alteration of the spectral signature. Since there is no other class to account for this altered signal it is classified as 'Tarmac' based on similarity. During the classification process a class to account for shaded signals was tested, but this lead to even higher confusion of classes, therefore it was removed again. The confusion of 'Tarmac' and 'Water' is due to the similarity of their natural spectral signatures. If there was no class accounting for tarmac, the paved roads in the study area would most likely be classified as water. This is the initial reason for the implementation of the 'Tarmac' class. Considering urban pixels, 28.1% were wrongly assigned to other classes, especially 'Bare Land' (compare table 4.1). The spectral signatures between bare land and urban structures are hard to distinguish as well. This is amplified due to other factors, such as buildings being constructed out of materials extracted from the local soil (Silver, 2014), as well as sand and soil covering areas of urban structures due to the local climate. Therefore the satellite captures a mixed signature, which makes the differentiation even harder. The classes 'Bare Land', 'Vegetation' and 'Water' were all classified reasonably well with accuracies ranging from 86.3% to 94.2%.

For further *usage* of the classification map, the user's accuracy is considered, since it shows how often the class in the map will represent the reality on the ground. Four out of the five classes show a user accuracy above 80%, with vegetation having the highest with a 99% accuracy. The high accuracies (both producer's and user's accuracy) of vegetation are most likely due to the added NDVI-layer, which helps to distinguish vegetation from other spectral signatures. The lowest user's accuracy can be found in the class of 'Tarmac', with 41.2% and a commission error of 58.8%. This ratio shows, that there is only a 41.2 chance of a pixel in this class representing the reality and a 58.8 chance of the 'Tarmac' pixel actually being water, bare land or urban. Therefore this class is not reliable and every conclusion based on this class is to be considered cautiously. The 'Urban' class on the other hand has a 81.5% reliability, and there is a 18.5 chance of the class not representing urban pixels, but rather bare land (see table 4.1). For further analysis this should be kept in mind.

The classification of the image from **2017** has an overall accuracy of 85.1% and a kappa of 0.790. Meaning the classification is significantly better than by mere chance. Same as in the image from 2008-2010 there are three of the five classes above an 80% producers accuracy. The class with the highest error of omission is 'Tarmac', with 45% of the tarmac pixels being wrongly classified into 'Bare Land' and 'Water' (compare table 4.2). The reasons for this are the same as for the 2008-2010 image. The 'Urban' class has an error of omission of 27.7%, with the highest number of wrongly classified pixels being assigned to 'Bare Land' and 'Tarmac', due to the similarity of spatial signatures and shade cast by buildings and clouds. Looking at the user's accuracy, 'Tarmac' has an error of commission of 78.1%, which is very high. This means there are more pixels in this class which belong into other classes, than pixels which actually represent tarmac. The error of commission of the class 'Urban' is 17.4%, therefore 82.6% of the 'Urban' pixels represent urban surfaces.

Table 4.2: Classification of 2017: Error Matrix (values in proportion to the total amount of sample points) and Accuracy Parameters; (1) - Bare Land, (2) - Vegetation, (3) - Urban, (4) - Tarmac, (5) - Water, Com U_i - Error of Commission, Om P_j - Error of Omission.

		Reference							
		(1)	(2)	(3)	(4)	(5)	Total	U_i	Com U_i
Map	(1)	0.388	0.005	0.058	0.000	0.003	0.453	0.857	0.143
	(2)	0.001	0.183	0.005	0.000	0.000	0.188	0.969	0.031
	(3)	0.040	0.002	0.217	0.004	0.000	0.263	0.826	0.174
	(4)	0.008	0.000	0.016	0.007	0.002	0.033	0.219	0.781
	(5)	0.000	0.000	0.005	0.002	0.056	0.063	0.895	0.105
	Total	0.437	0.189	0.300	0.013	0.061	1		
	P_j	0.888	0.966	0.723	0.550	0.920		O	0.851
	Om P_j	0.112	0.034	0.277	0.450	0.080		Kappa	0.790

It can be concluded that most classes were reasonably well classified, except the class of 'Tarmac'. Since the total area of the 'Tarmac' class is comparably small, the error does not nessesarily effect the other classes notable. Considering the 'Bare Land', 'Vegetation' and 'Urban' class, both the user's and producer's accuracies are each very similar for both time frames, therefore the results are comparable. In general it is important to realize, that a classification can only show what the analyst knows and the accuracy assessment is tied to the land cover interpretation of the analyst.

4.2 Urban Land Cover Growth in almost a Decade

The resulting images of both random forest classifications (and subsequent reclassification) are displayed and discussed in the following (see fig. 4.1 for 2008-2010 and fig. 4.3 for 2017).

In **2008-2010**, the largest land cover is bare land with 42.5 km^2, followed by vegetation with 21.3 km^2, while the smallest is tarmac with 2.0 km^2 (see table 4.3). The extent of the urban area in 2008-2010 is calculated to be 19.2 km^2. Inspecting the classified image there are some things

Table 4.3: Extent of each class in the study area as well as in each district in 2008 - 2010 (areas of Ga Central Municipal are neglected)

	Bare Land	Vegetation	Urban	Tarmac	Water	Total
Study Area	42.5 km^2	21.3 km^2	19.2 km^2	2.0 km^2	6.9 km^2	91.9 km^2
Ga South	27.5 km^2	18.7 km^2	8.7 km^2	1.0 km^2	5.4 km^2	61.3 km^2
Accra Metropolis	14.7 km^2	2.6 km^2	10.4 km^2	1.0 km^2	1.3 km^2	29.9 km^2

that are recognizable right away. It is visible that the Densu river is flowing from the Weija lake south to the Densu delta, where parts of the image in between are unfortunately lost due to

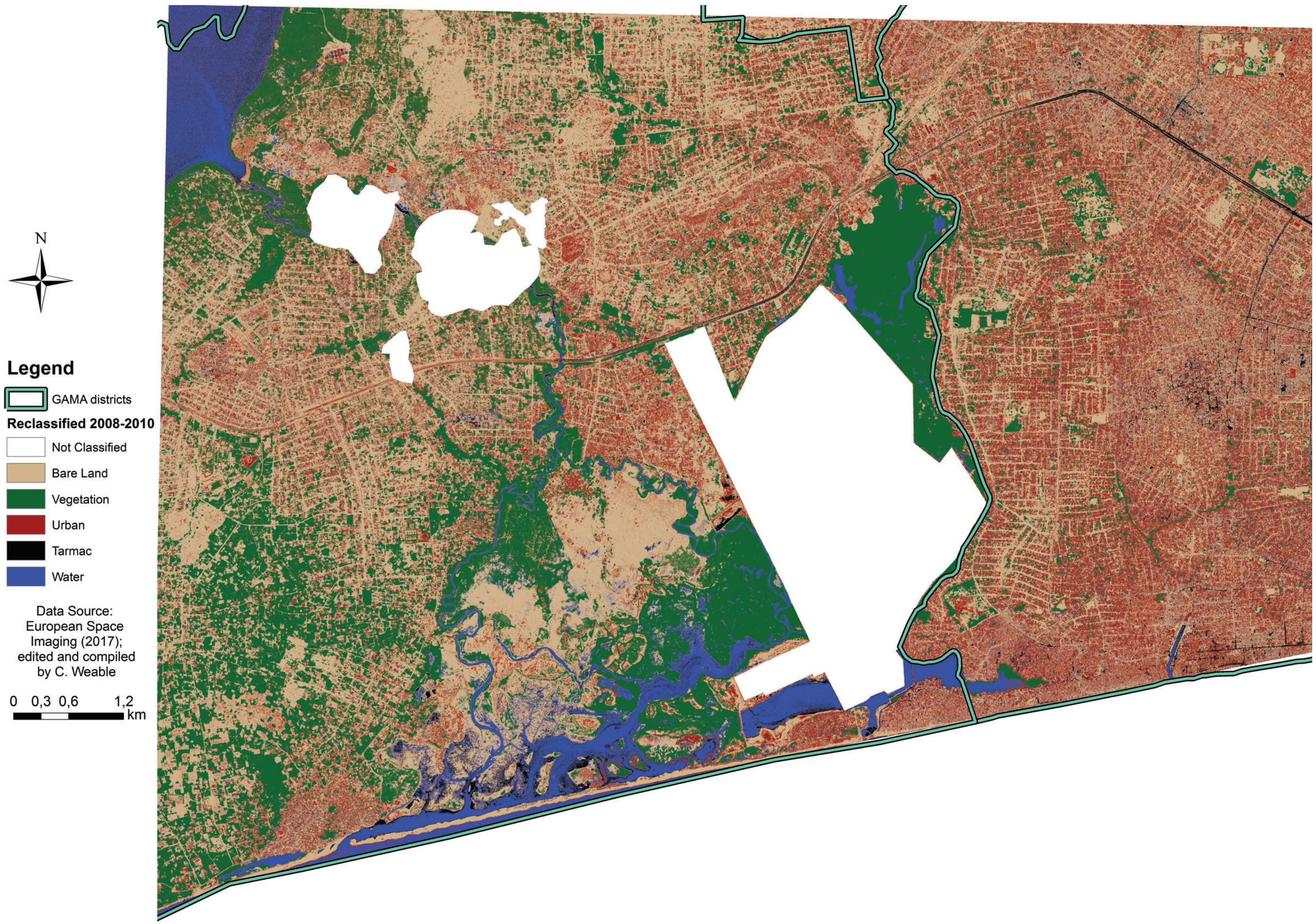

Figure 4.1: Land cover status of 2008-2010, classified through random forest classification.

cloud coverage. The Densu delta is characterized through a strong mixture of different classifications, mainly vegetation, water and bare land, as well as some scattered wrongly classified urban pixels. These abrupt discontinuities are due to the fixed classes and do not reflect the natural environmental gradients between these classes. The small informal settlement Tetegu inside the Densu delta is also clearly visible. Even the Weija Water works in the north-west of the image were identified as small concentric circles with a water signature. Focusing back on the urban class, the higher frequency of the urban pixels seems to be in the eastern part of the image (i.e., AMA). This is confirmed by the calculated urban extent inside AMA[2] being 10.4 km^2, whereas Ga South, although with a higher total area, only has an urban coverage of 8.7 km^2 (see table 4.3). Inside AMA there are a few larger vegetation patches, which are due to the Accra Academy and the Wesley Grammar Senior High School. Staying in the east, the Winneba Rd is partially identified as tarmac. Although the accuracy of this class is not reliable, the tarmac pixels unmistakably represents the shape of the Winneba Rd. Following this road, to the west side of the image, the urban pixels give the impression of being located in proximity to the street. Moving south of Winneba Rd there are progressively less urban pixels. West of the Densu delta along the shore line the village Tsokomey (Bortianor) is visible. In this image, the village is only connected to the main road (Winneba Rd.) through a long curvy street with the signal of bare land. It also appears that different parts of the city have different urban textures. Incorporating textures in the method could therefore be a point of further research. Moreover, some areas have clear straight roads in rectangular arrangement, while in other places no clear pattern is distinguishable (as in Glefe, SE of the delta), which suggests a lack of urban planning in these areas (Grant & Yankson, 2003).

Comparing the land cover extents of the two districts Ga South and Accra Metropolis is best done in ratios, since both have different total extents represented in the image (see fig. 4.2). It is evident, that the ratio of bare land does not vary much between the two districts, but especially the ratios of vegetation and urban differentiate substantially. The proportional urban land coverage is much smaller in Ga South than in Accra Metropolis. At the same time the vegetation coverage is much higher.

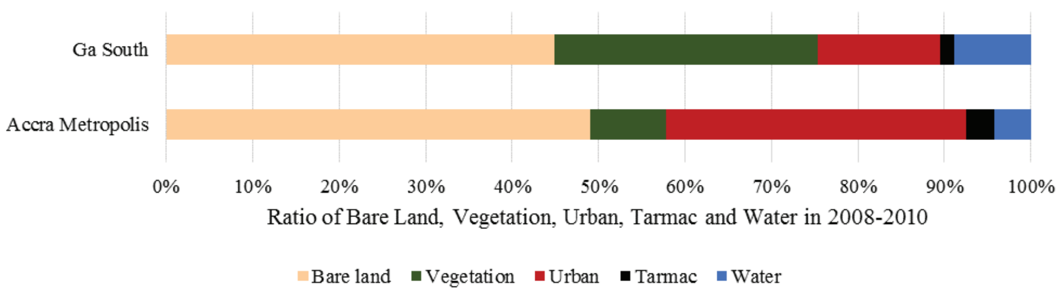

Figure 4.2: Land cover ratio of bare land, vegetation and urban in 2008-2010 in the two districts

[2]While comparing the extents of classes in both districts, it should be noted that only the area of the districts inside the study area are considered, since that is the extend of the data.

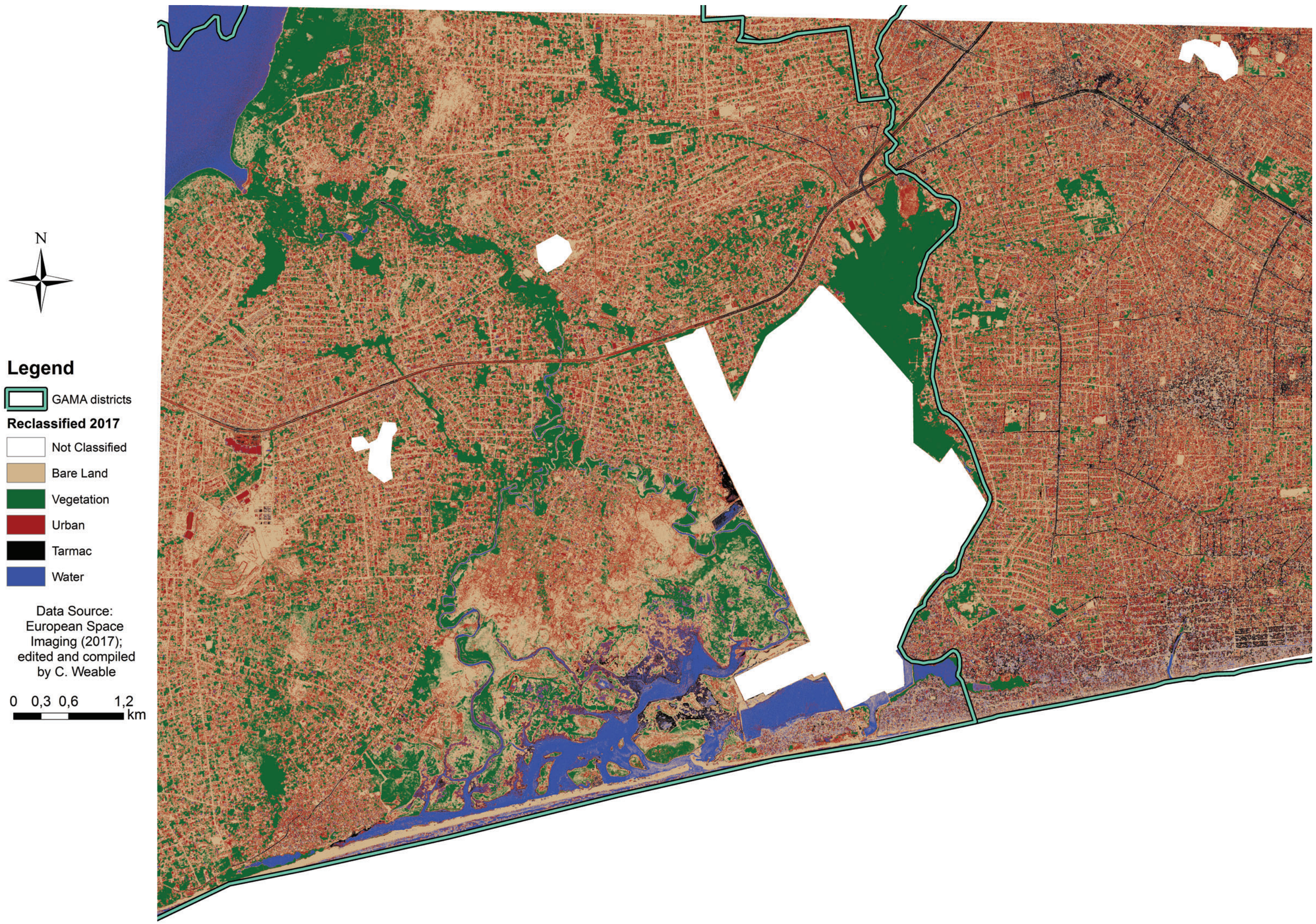

Figure 4.3: Land cover status of 2017, classified through random forest classification

In the **2017** image the largest area is, same as in 2008-2010, bare land with 42.3 km^2 (in 2008-2010 it was 42.5^2), followed now by urban with an extent of 24.6 km^2 (in 2008-2010 it was 19.2 km^2). The increase of urban pixels in comparison to 2008-2010 is also visually noticeably. Vegetation covers only 17.6 km^2 in 2017, while in 2008-2010 it covered 21.3 km^2. Some observations from the classified image out of 2017 are different than 2008-2010. The Densu river is not as visible, as it was before. It either seems to be covered with vegetation, or the water flow is so low that the vegetation signal is more dominant than the water signal. More information is needed to tell if this is as a result of seasonal changes or if the water flow in general has decreased. Moreover, in regards to urban coverage, the coverage around the informal settlement Tetegu has expanded noticeably. Likewise the area around the coastal settlement Tsokomey (Bortianor) has distinctly more urban coverage.

Table 4.4: Extent of each class in the study area as well as in each district in 2017 (areas of Ga Central Municipal are neglected)

	Bare Land	Vegetation	Urban	Tarmac	Water	Total
Study Area	42.3 km^2	17.6 km^2	24.6 km^2	3.1 km^2	5.6 km^2	93.5 km^2
Ga South	27.9 km^2	15.0 km^2	14.7 km^2	0.7 km^2	4.6 km^2	63.0 km^2
Accra Metropolis	14.1 km^2	2.6 km^2	9.7 km^2	2.4 km^2	1.0 km^2	29.8 km^2

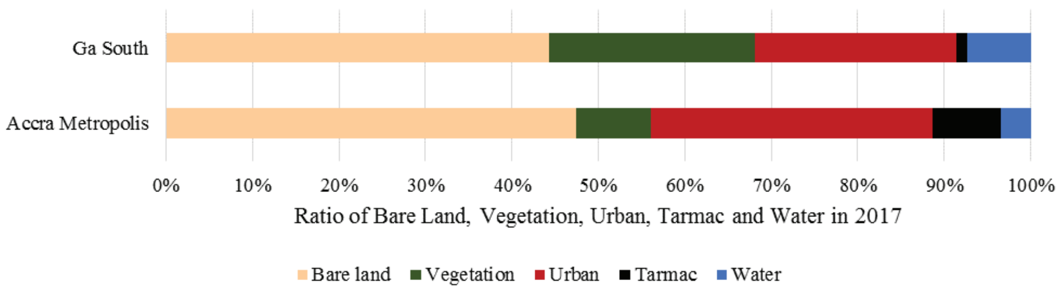

Figure 4.4: Land cover ratio of bare land, vegetation and urban in 2017 in AMA and Ga South

Comparing the land cover coverage ratios of both districts, the general distribution of the coverage is similar to 2008-2010. In Ga South urban land cover has increased, while vegetation has decreased. To examine a more detailed distribution of land cover in the districts an analysis using a fishnet (see chapter 3.4) was conducted. In the following image (4.5) the ratios of the three classes (bare land, vegetation and urban) are plotted in a Ternary diagram. The distribution of the ratios is distinctly different in both districts. While most of the areas in AMA show an urban ratio of above 30%, the majority of areas in Ga South show an urban ratio below 30%. In addition to this is the vegetation ratio of AMA mostly under 20%, whereas in Ga South there are more areas with a much higher vegetation ratio. There are also several outliers for both districts. These are due to some squares only covering a very small area of the classification map and therefore the ratios are distorted. For example there are two outliers which display to represent a 0% vegetation share, while having over 60% and 80% urban coverage. These two are squares, which cover a small area along the coast (near Glefe) with only sand and urban land cover. This leads to the distortion. Since there are only very few of these outliers, the general tendency of the land coverage is still identifiable.

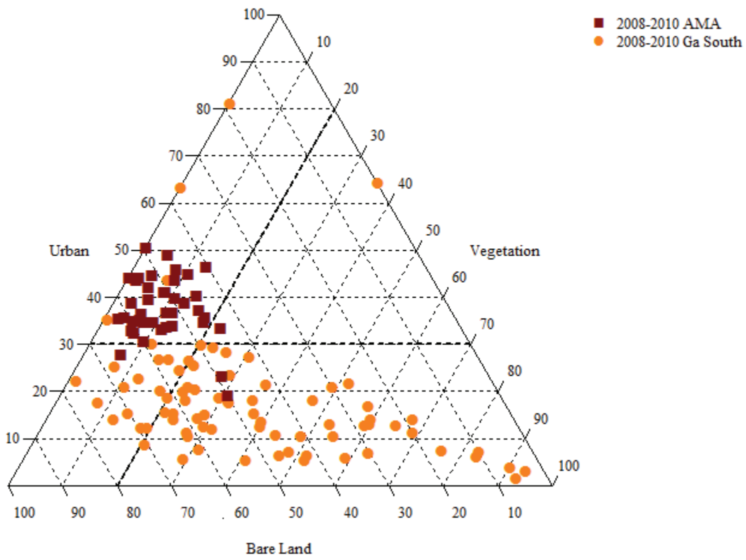

Figure 4.5: Ternary diagram of AMA and Ga South in 2008-2010. Plotted are 121 ratios (Bare land, urban and vegetation) where 41 represent AMA and 80 represent Ga South.

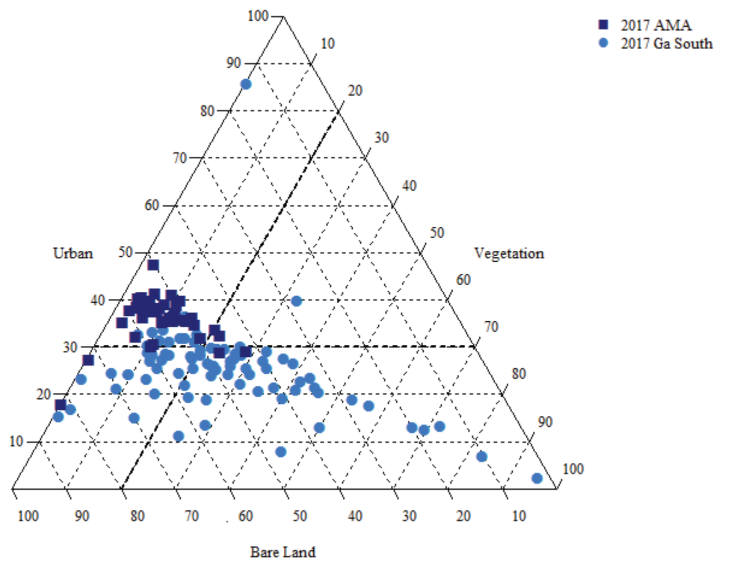

Figure 4.6: Ternary diagram of AMA and Ga South in 2017. Plotted are 121 ratios (Bare land, urban and vegetation) where 41 represent AMA and 80 represent Ga South.

So essentially the plot of the three ratios shows that the composition of urban, bare land and vegetation is fairly different between the two districts. Therefore the result of this comparison is the confirmation of variations between both districts. In the figure (4.6) the same ratios are plotted per district based on the results of the classified image from 2017. For the distribution of the same areas in 2017 a similar tendency is visible. Here the areas of AMA show an urban ratio higher than 30% and a vegetation ratio mostly below 20% as well. For Ga South the urban ratio appears to be dominantly beneath 30%. However, the areas of Ga South have slightly moved upward in the plot (higher density at the 30% line), which means an increase in urbanization has taken place. The vegetation ratio on the other hand seems to be less distinctly above 20% than in 2008-2010. Nonetheless, a clear differentiation in composition is still visible between both districts. Since the land coverage of bare land appears to stay above 40% for the majority of areas, the trade-off of a growing urban extent seems to be vegetation coverage. To examine the changes in land cover and especially the trade-offs in more detail, a change detection is calculated.

4.3 Patterns of Urban Land Cover Growth

The results of the matrix union to identify change are shown as a change detection matrix below (table 4.5). The change detection matrix shows how much area has stayed the same class over the analyzed decade and how much area has changed. According to these results 43.73 km^2

Table 4.5: Change Detection Matrix

2008-2010 / 2017	Bare Land	Vegetation	Urban	Tarmac	Water	Total
Bare Land	*23.46 km^2*	5.13 km^2	11.96 km^2	1.63 km^2	0.98 km^2	43.17 km^2
Vegetation	7.72 km^2	*9.42 km^2*	4.01 km^2	0.19 km^2	0.44 km^2	21.77 km^2
Urban	8.93 km^2	1.93 km^2	*7.24 km^2*	0.78 km^2	0.67 km^2	19.56 km^2
Tarmac	0.66 km^2	0.08 km^2	0.37 km^2	*0.33 km^2*	0.59 km^2	2.03 km^2
Water	1.73 km^2	0.67 km^2	1.07 km^2	0.26 km^2	*3.28 km^2*	7.00 km^2
Total	42.50 km^2	17.23 km^2	24.66 km^2	3.19 km^2	5.96 km^2	93.54 km^2

have stayed the same and 49.81 km^2 have changed. Looking at each class individually, bare land had a net decrease of 0.7 km^2, while vegetation had a net decrease of 4.5 km^2. Water also shows a net decrease of 1 km^2. Urban and tarmac on the other hand increase by 5.1 km^2 and 1.2 km^2. As shown in the accuracy assessment the class of tarmac is not reliable, therefore it can be assumed that area from this class should be added to another class such as urban and water. Since all of these values are relatively similar, the error of falsely classified tarmac could change the net change of another class considerably. As to the trade-offs of land cover classes: Focusing on Urban, in 2008-2010 the urban area had an extent of 19.56 km^2 and in 2017 an extent of 24.66 km^2 in this calculation, which differs slightly from the extent calculations seen in table 4.3 (19.2 km^2) and 4.4 (24.5 km^2). These discrepancies are most likely rounding errors from the different calculation steps. Furthermore, the change detection matrix implies a loss of 11.96 km^2 of bare land to urban but at the same time a gain of 7.72 km^2 from vegetation. This standing by itself, would imply a chain of urban claiming bare land, which has the effect of turning vegetation into bare land. However at the same time vegetation gains 5.13 km^2 from bare land over the same time period, which seems contradictory. With the intention of clearing up this inconclusive trade-off of land covers, the spatial distribution of the changed pixels were visually analyzed. Unfortunately there were no patterns detectable which could shed light upon processes lying beneath the land cover trade-offs (see appendix table A.3). One interesting observation that could be made was the expansion of tarmac roads from 2008-2010. Although the tarmac class has a low accuracy, the patterns of streets extending from Winneba Rd. and the core of AMA were distinctively visible. There were certainly also many pixels, especially in Glefe, which could be falsely classified as tarmac, nevertheless the expansion of tarmac roads is clearly identifiable (see appendix fig. A.3). In summation, the change detection matrix does not give much information which helps to identify land cover change processes. This might be due to the pre-processing, such as the geometrical correction. The geometrical correction was done to ensure the pixels of one time frame would be situated at the exact location of the pixels in the second time frame. This should prevent the measurement of a change, as a result of askew pixel locations. Through the geometrical correction however, the pixel size was modified. Therefore it seems likely that the pixels do not cover the same area, which would then again lead to a false change detection. As these results did not lead to the satisfactory results one was hoping for, in further research different change detection techniques, such as principal component analysis or change vector analysis could be used (Almutairi & Warner, 2010).

Regardless of the change detection matrix result, the overall change in land cover can show the tendencies in which the land cover of the study area has changed over the last decade. In the following table 4.6 the magnitude and percentage of land cover change is shown. For this the

Table 4.6: Magnitude and percentage of land cover change from 2008-2010 to 2017

Class	2008-2010		2017		Change	Total	Per Year
Bare Land	42.5 km^2	46.2%	42.3 km^2	45.3%	-0.2 km^2	-0.42%	-0.05%
Vegetation	21.3 km^2	23.2%	17.6 km^2	18.8%	-3.7 km^2	-17.46%	-2.37%
Urban	19.2 km^2	20.9%	24.6 km^2	26.3%	5.3 km^2	27.76%	3.11%
Tarmac	2.0 km^2	2.2%	3.1 km^2	3.3%	1.1 km^2	56.64%	5.77%
Water	6.9 km^2	7.5%	5.9 km^2	6.3%	-1.0 km^2	-14.55%	-1.95%
Total	91.9 km^2	100%	93.5 km^2	100%			

proportion of each class extent from each time frame (table 4.3 and 4.4) in relation to the total extent was calculated, as well as the difference of each class and the related growth rate. This shows an overall growth rate of 27.76% for urban land cover in almost a decade and an annual growth rate of 3.11%. The largest annual land cover loss is the vegetation with -2.37%, followed by water with -1.95%. Bare land on the other hand only shows a slight decline of -0.05%. The two larger water bodies north of the Panbros salt ponds disappeared and changed into vegetation in the course of seven years, which explains the shrinkage of water land cover.

Going back the ratio of urban, bare land and vegetation, fig. 4.7 displays how the composition of the entire classified image has changed over time. In this plot a higher density, especially for 2017, can bee seen around 25 to 40% urban and 5 to 20% vegetation. The areas from 2008 seem to be more widely distributed, especially with less urban and higher vegetation. Nevertheless there are also areas with more urban land cover than in 2017. To inspect the changes in more detail, a separate analysis of both districts could help.

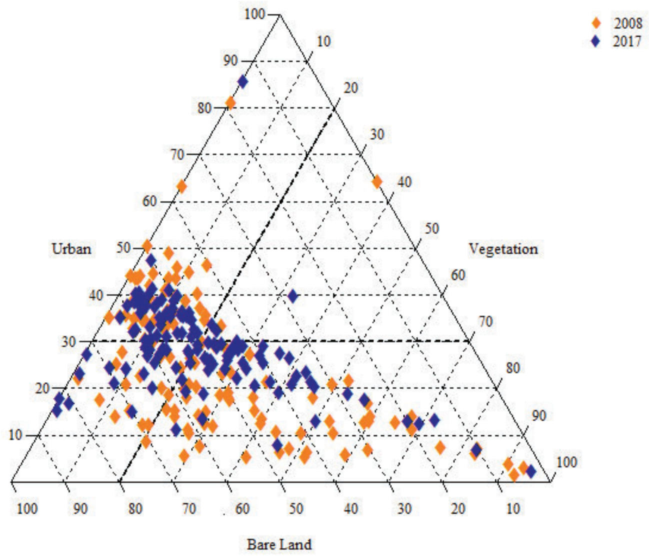

Figure 4.7: Ternary diagram of Study Area from 2008-2010 and 2017. Plotted are 242 ratios (bare land, urban and vegetation) where 121 represent the study area in 2008-2010 and 121 represent the study area in 2017.

While the inspection of the Ternary plot shows the areas located in AMA over time (fig. 4.8), it is apparent that for both time frames the composition does not vary much. In both time frames the vegetation ratio is mostly under 20% and the urban ratio over 30%. Nonetheless, there are areas which appear to have a higher urban ratio in 2008-2010, than 2017. To explain this phenomenon the original data was consulted. The most likely explanation is that in 2017 urban pixels in these exact areas were categorized as tarmac, therefore the ratio of urban is decreased in comparison to 2008-2010, especially if only three out of five variables are considered. This is confirmed, when comparing the urban extent in AMA in 2008-2010 (table 4.3) with 10.4 km^2 and the urban extent in AMA in 2017 (table 4.4) with 9.7 km^2. There has not actually been a decrease in urban area, it is just that some streets in 2008 have a urban signature and have been paved with tarmac, while other areas have been falsely classified as tarmac due to shadow and moisture, although they should belong to the urban class. The absence of differentiation in composition (in the Ternary diagram) can also be interpreted as the absence of further urban growth. As stated in chapter 2.4, the population growth in AMA has been consistently under 1, which also reflects a slow growth. Although there are indices to calculate the Annual Urban Expansion Rate ($AUER_i$), the meaningfulness of these would be undermined due to Ga South and AMA only being partially included in the study area. This would also mean that they are not comparable with other expansion rates. Another aspect, which is important to remember at this point, is the fact that only the actual soil sealing (spatial extent) is measured with this method, therefore all aspects of expanding urban structures on the vertical axis (in height, etc.)

can not be measured using this technique. Hence a population growth is possible, even if the urban extent does not grow in the same manner.

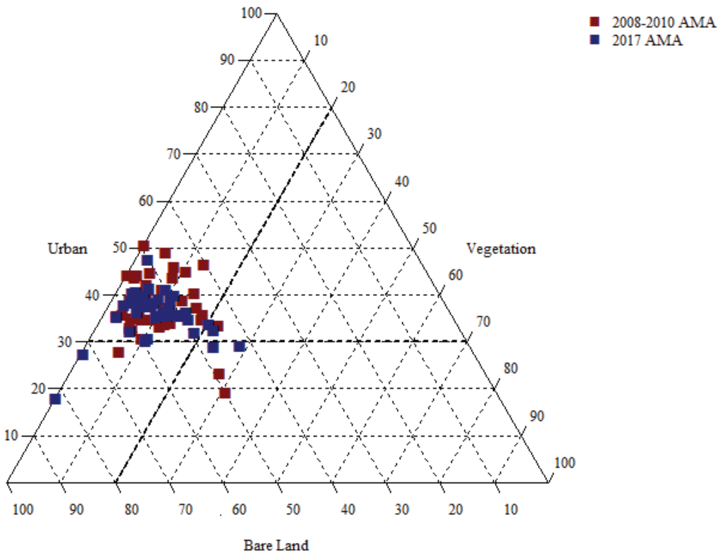

Figure 4.8: Ternary diagram of AMA from 2008-2010 and 2017. Plotted are 82 ratios (Bare land, urban and vegetation) where 41 represent AMA 2008-2010 and 41 represent AMA 2017.

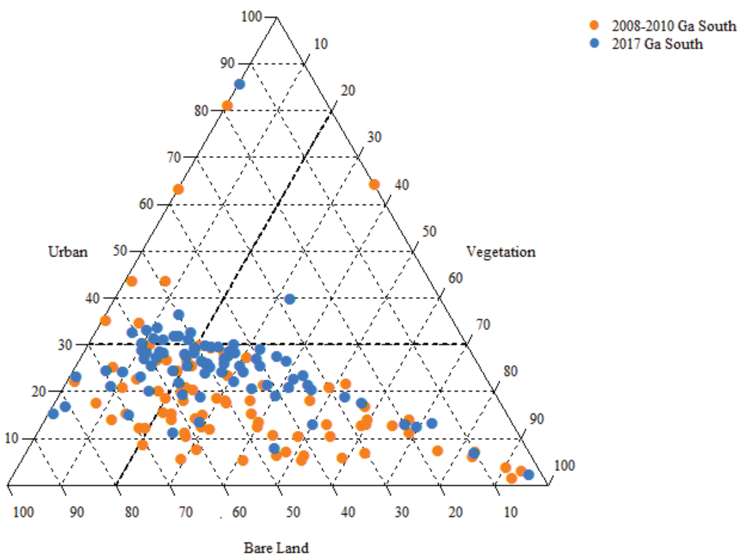

Figure 4.9: Ternary diagram of Ga South from 2008-2010 and 2017. Plotted are 160 ratios (Bare land, urban and vegetation) where 80 represent Ga South 2008-2010 and 80 represent Ga South 2017.

As for the change in Ga South (fig. 4.9), the compositions from each time frame differ substantially. In 2017 the urban ratio is comparatively higher than in 2008-2010, which is expected at this point. The plotted areas give the impression of moving toward the intersection of the highlighted vegetation and urban line. Nevertheless, only a few have crossed the 30% urbanization line, while many more have crossed the vegetation line below 20%. Since bare land stays mostly constant, the composition points seem to move along those lines. Here again, the data gives the impression, that the main trade-off happens between vegetation and urban. "An increase in urban structures and a decrease in vegetation cover usually characterizes development" (Seto et al., 2002).

Nevertheless, since these diagrams show how districts can change through different stages, the method of plotting this type of composition could help determine in what stage a district or area is at any given point in time, provided there is satellite imagery available. Since there is ongoing research in the field of defining the peri-urban in contrast to urban or even rural, this method could help in regards to the spatial distribution of land cover (Simon, McGregor, & Nsiah Gyabaah, 2004). There are many ways to define the urban, rural and peri-urban, as stated by Simon et al. (2004). If the factors which can not be measured from the air, such as 'access to markets', 'ready supply of labor' and 'pollution', are set aside, one could use these plots to determine if an area is urban or rural or even peri-urban based on the degree of soil sealing, which would reflect a degree of development. In many literature, including Doan and Oduro (2012), AMA is consider city center and therefore it would be urban. Ga South on the other hand is mostly considered to be peri-urban. Peri-urban is often said to be a transitional zone between the city and the country side and consequently considered both urban and rural (Salem, 2016). This corresponds to the results shown in the Ternary diagrams presented above. Interpreting the results in this manner means that Ga South is moving from a former rural area through a peri-urban development at the moment, towards a urban development. There has been some evidence found [3], which suggests that cities expand according to a development cycle (Dreyer, 2017). Dreyer also states, that it will likely by a trend in many African cities. Through analysis of more areas and plotting the resulting compositions in a Ternary diagram this method could show to help with defining areas as urban, rural or peri-urban.

Regarding the analysis of the four areas to check the hypothesis on patterns of population growth (Doan & Oduro, 2012), the results are shown in the following figure (4.10). Unsurprisingly all four areas show an increase in urban ratio. Interesting is the fact, that area 2 (h2) and 3 (h3) mainly show a decrease in vegetation (both >10%), while for area 1 (h1) and 4 (h4) the vegetation ratio is relatively stable and the bare land ratio decreases (both >10%). This again shows that there is not one big trade-off, but that it very much depends on the area and scale of observation. Although the areas start at slightly different ratios of urban (between 10 and 20%), they all end up with an urban ratio near 30%. In relation to the results of Doan and Oduro (2012), the more general hypothesis of the spreading pancake can mostly be confirmed with the data at hand, since all analyzed areas can record an increase in urban land cover. Nevertheless, when comparing the change from the area closest to the city to the area furthest away, as the first hypothesis would suggest, there is no pattern to be found. This confirms that there are more facets to the urbanization process, since the total proximity to the main city does not independently determine the urbanization process, but other aspects as well, such as the other three hypothesis. As for the second area (h2) and the associated development node hypothesis, a significant urbanization

[3] This was research of a Master Thesis by Zachary Dreyer at the Trier University in 2017

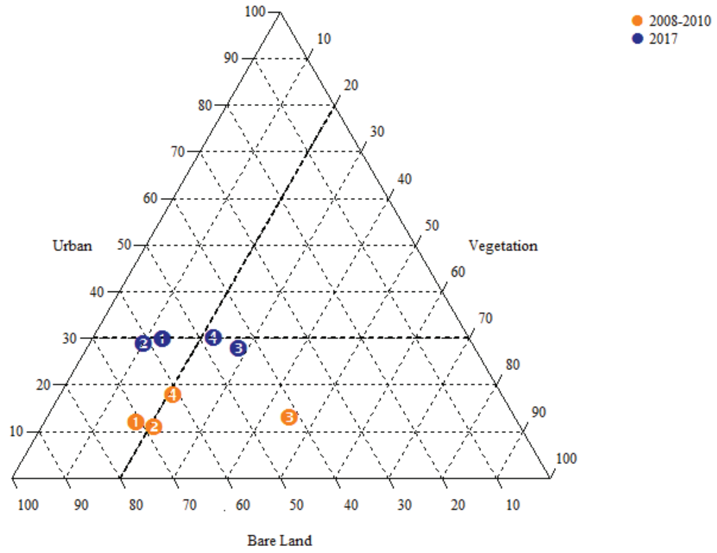

Figure 4.10: Ternary diagram of the hypothesis analysis. Each orange point stands for the hypothesis it analyses in 2008-2010 and each blue point for the according area in 2017. 1 - Spreading pancake hypothesis, 2 - Development node hypothesis, 3- Village magnet hypothesis, 4 - Ribbon hypothesis

increase can be found. Although the data confirms this hypothesis, the relation of data to the process does not exist, which makes a total conformation of this hypothesis difficult. The effect of urbanization growth can be measured, but with the means at hand the direct linkage to the process is not possible. The same goes for the other two hypotheses, where in both areas an increase of urban growth can be found, but the linkage to the process is not actionable. This difficulty of linking both quantitative measurements and process is the same as in the original paper by Doan and Oduro (2012) as well, since there analysis is based on population data. To conclusively link the both of them a more in depth human geography or social science approach is needed. But the need and the exact areas for this research can be based off of the results presented in both analyses.

In summation, this analysis displays how single areas have changed over time and that a general increase in urban land cover has occurred, but the direct linkages between the process and the measurable result need further research, from a in depth human geography or social science approach.

5 | Conclusion and Outlook

Summarizing, the classification method random forest proved to work fairly well for this analysis with an overall accuracy of 0.864 for 2008-2010 and 0.851 for 2017. Nevertheless, there is also room for improvement. With even more time one could fine tune the classification and the sample points even more, especially to improve the classification of tarmac. As for the land cover status of 2008-2010 a clear distinction between AMA and Ga South is detectable. AMA has an urban cover of 0.35 km^2 per square kilometer, while Ga South has an urban cover of 0.14 km^2 per square kilometer in 2008-2010. For 2017 the urban cover in AMA has mostly stayed the same with 0.33 km^2 per square kilometer (small loss due to increase in tarmac), but Ga South records an increase of urban cover to 0.23 km^2 per square kilometer. This adds up to a total increase of 27.76% urban land cover and an increase of 3.11% annually. In the change detection analysis no direct trade off between land covers could be detected, nonetheless, this could be subject to further research.

As to the detection of patterns, through the use of Ternary diagrams the composition of the ratios from bare land, vegetation and urban land covers can be used to distinguish between different degrees of soil sealing. In this case study the district of the city center (AMA) has leveled at a certain degree of soil sealing, while a district belonging to the urban exterior (Ga South) shows tendencies moving towards the same degree of soil sealing. Through the inclusion of the variables vegetation and bare land the overall trade off per area can be detected as well. The composition of the three variables can help describe areas and also help define urban areas. Testing this method on other areas would further the research of this method and validate if this method can also be used in other study areas.

In this context, the research project "Analysis of two streets in the Densu Delta using Mapping Keys" showed how development on the scale of two streets can variate. The research illustrates how the development degree varies based on the urban structures found in these streets (Weable, 2018). This shows that there are always different development degrees and what definitions and measurements are used is dependent on the scale of interest. Looking at different scales and how the ratio approach holds up at each scale could also be an interesting research to follow up this thesis.

The next step of this research was the analysis of four hypotheses describing different forms of urbanization, caused by different drivers. All four areas, each representing one hypothesis, show an increase in urban extent. Unfortunately, no real distinction in the results could be made between all four areas. Therefore the first hypothesis, claiming that cities spread like pancakes, appears to be validated, due to gradient of urban coverage from East (h1 and h4 in fig.3.2 and fig.4.10) to West (h3 and h2 in fig. 3.2 and fig.4.10). Nevertheless, the linkage of increased urban extent to the process behind the hypotheses, such as economic benefits or commuting benefits, is not possible. For this further in depth research, focusing on social aspects, is needed. Nonetheless, this could be a great linkage point of both disciplines. Based on the quantitative data gained through remote sensing analysis, a qualitative analysis could follow, focusing on linking the quantitative results with the processes and drivers underneath.

Remote sensing of cites is a relatively new field, which is advancing more quickly through higher resolution and higher general data quality (Xiuwan, 2002). Nevertheless, in the end, this type of research does not necessarily require more precise data, but a better understanding (Frick-Trzebitzky, 2017). A better understanding of what information methods can and can not provide and a better understanding of what urban science consists of. Since the goal of this thesis was an interdisciplinary approach of detecting urbanization patterns, not only should the analyzed patterns be summarized and reflected on, but also the interdisciplinary approach itself. Although both disciplines have many overlaps, topic-wise and otherwise, combining both approaches in one analysis can be challenging, due to its complexity. "Much of the complexity in urban remote sensing studies is due to the simple fact that urban growth itself is a complex" (Dreyer, 2017; Huang, Lu, & Sellers, 2007). As presented in this thesis, there are many ways to approach such a complex topic. Urban development is influenced and steered by social phenomena, which are related to the context within which the phenomena is situated. Contexts are measured in various ways, such as Censuses and social network analyses (Rindfuss & Stern, 1998). Remote sensing provides yet another way of gathering contextual data, especially biophysical context. In this thesis the contextual data was the identification of urban development in parts of AMA and Ga South. Remotely sensed data provides an alternative representation for geographical context, such as maps. Maps aim to show the reality, however, maps mostly show the mapmaker's selection of what is important to represent and therefore can include different biases (Rindfuss & Stern, 1998). This is a key aspect to consider. This is why interdisciplinary work is very important. The results of remote sensing analysis should aim to help understand processes and social phenomena, especially in regards to urban science. For this research the results show a differentiation of urban development through percentage of soil sealing. By means of using the Ternary plot, the different degrees of soil sealing (in relation to vegetation and bare land) can be visualized and potentially, through further research, thresholds could be considered. Nevertheless, the results of this research are not sufficient to determine the exact urban form (e.g. peri-urban, etc.) of an area, since there are many factors involved which also have to be considered and can not be measured from the air.

There is also still a lot of potential in the results of the classification, which hasn't been used yet and could be used in further research. However, analysis like this can give a good quantitative data basis for research in human geography and social science. For this to work the remote sensing analyst needs to understand how his definitions and interpretations of the phenomenons associated with the analysis affect the outcome of the research, which in turn influences all further research. At the same time the human geographer need to understand, where the used data comes from and what biases might be implied in them. And this is how both disciplines depend on each other and further interdisciplinary work.

Bibliography

Acuto, M., Parnell, S., & Seto, K. C. (2018). Building a global urban science. *Nature Sustainability*, *1*, 2–4. doi:10.1038/s41893-017-0013-9

Affam, M. & Asamoah, D. N. (2011). Economic Potential of Salt Mining in Ghana Towards the Oil Find. *Research Journal of Environmental and Earth Sciences*, *3*(5), 448–456.

Akubia, J. E. (2018). Conversation about GAMA shapefile.

Almutairi, A. & Warner, T. A. (2010). Change detection accuracy and image properties: A study using simulated data. *Remote Sensing*, *2*(6), 1508–1529. doi:10.3390/rs2061508

Angel, S., Blei, A. M., Parent, J., Lamson-Hall, P., & Sánchez, N. G. (2016). *Atlas of Urban Expansion - 2016 Edition, Volume 1: Areas and Densities*. New York: New York University, Nairobi: UN-Habitat, and Cambridge, MA: Lincoln Institute of Land Policy. doi:10.5860/CHOICE.50-1227

Badmos, O., Rienow, A., Callo-Concha, D., Greve, K., & Jürgens, C. (2018). Urban Development in West Africa—Monitoring and Intensity Analysis of Slum Growth in Lagos: Linking Pattern and Process. *Remote Sensing*, *10*(7), 1044. doi:10.3390/rs10071044

Bartels, L. E., Bruns, A., & Alba, R. (2018). The production of uneven access to land and water in peri-urban spaces: de facto privatisation in greater Accra. *Local Environment*, *Nov*(11), 1–18. doi:10.1080/13549839.2018.1533932

Belgiu, M. & Drăgu, L. (2016). Random forest in remote sensing: A review of applications and future directions. *ISPRS Journal of Photogrammetry and Remote Sensing*, *114*, 24–31.

Boyle, S. A., Kennedy, C. M., Torres, J., Colman, K., Pérez-Estigarribia, P. E., & De La Sancha, N. U. (2014). High-resolution satellite imagery is an important yet underutilized resource in conservation biology. *PLoS ONE*, *9*(1), 1–11. doi:10.1371/journal.pone.0086908

Brannen, J. (1992). Combining qualitative and quantitative approaches: an overview. In *Mixing methods: Qualitative and quantitative research* (pp. 3–37). London: Routledge.

Breiman, L. (2001). Random Forests. *Machine Learning*, *45*(1), 5–32. doi:10.1023/A:1010933404324

Broich, M., Hansen, M. C., Potapov, P., Adusei, B., Lindquist, E., & Stehman, S. V. (2011). Time-series analysis of multi-resolution optical imagery for quantifying forest cover loss in Sumatra and Kalimantan, Indonesia. *International Journal of Applied Earth Observation and Geoinformation*, *13*(2), 277–291. doi:10.1016/j.jag.2010.11.004

Cobbinah, P. B., Gaisie, E., & Owusu-Amponsah, L. (2015). Peri-urban morphology and indigenous livelihoods in Ghana. *Habitat International*, *50*, 120–129. doi:10.1016/j.habitatint.2015.08.002

Cohen, B. (2006). Urbanization in developing countries: Current trends, future projections, and key challenges for sustainability. *Technology in Society*, *28*(1-2), 63–80. doi:10.1016/j.techsoc.2005.10.005. arXiv: arXiv:1011.1669v3

Coppin, P., Jonckheere, I., Nackaerts, K., Muys, B., & Lambin, E. (2004). Digital change detection methods in ecosystem monitoring : a review. *International Journal of Remote Sensing*, *25*(9), 1565–1596. doi:10.1080/0143116031000101675

Cowen, D. J., Jensen, J. R., Bresnahan, P. J., Ehler, G. B., Graves, D., Huang, X., ... Mackey, H. E. (1995). The Design and lmplementation of an lntegrated Geographic lnformation

System for Environmental Applications. *Photogrammetric Engineering & Remote Sensing*, *61*(11), 1393–1404.

Doan, P. & Oduro, C. Y. (2012). Patterns of population growth in peri-urban accra, ghana. *International Journal of Urban and Regional Research*, *36*(6), 1306–1325. doi:10.1111/j.1468-2427.2011.01075.x

Dreyer, Z. (2017). *Assessing Patterns of Urbanization in Developing Countries Using Landsat Image Composites and Spectral Mixture Analysis : A Case Study From Menongue, Angola* (Doctoral dissertation, Trier University).

Du, X., Jin, X., Yang, X., Yang, X., & Zhou, Y. (2014). Spatial pattern of land use change and its driving force in Jiangsu province. *International Journal of Environmental Research and Public Health*, *11*(3), 3215–3232. doi:10.3390/ijerph110303215

EEA. (1994). CORINE land cover - contents. *CORINE land cover*, 1–163. doi:10.1111/j.1420-9101.2010.02187.x

European Space Imaging. (2017). Products and Services. Retrieved July 9, 2018, from http://www.euspaceimaging.com/products

Finlayson, C., Gordon, C., Ntiamoa-Baidu, Y., Tumbulto, J., & Storrs, M. (2000). The hydrobiology of Keta and Songor lagoons : implications for coastal wetland management in Ghana.

Fisher, J. R. B., Acosta, E. A., Dennedy-Frank, P. J., Kroeger, T., & Boucher, T. M. (2017). Impact of satellite imagery spatial resolution on land use classification accuracy and modeled water quality. *Remote Sensing in Ecology and Conservation*. doi:10.1002/rse2.61

Foody, G. M. (2002). Status of land cover classification accuracy assessment. *Remote Sensing of Environment*, *80*, 185–201. doi:10.1016/S0034-4257(01)00295-4

Franklin, S. E., Ahmed, O. S., Wulder, M. A., White, J. C., Hermosilla, T., & Coops, N. C. (2015). Large Area Mapping of Annual Land Cover Dynamics Using Multitemporal Change Detection and Classification of Landsat Time Series Data. *Canadian Journal of Remote Sensing*, *41*(4), 293–314. doi:10.1080/07038992.2015.1089401

Frick-Trzebitzky, F. (2017). GIS – what can and what can't it say about social relations in adaptation to urban flood risk? (15). WaterPower Working Paper. Governance and Sustainability, Trier University. Trier.

Frick-Trzebitzky, F., Baghel, R., & Bruns, A. (2017). Institutional bricolage and the production of vulnerability to floods in an urbanising delta in Accra. *International Journal of Disaster Risk Reduction*, *26*, 57–68. doi:10.1016/j.ijdrr.2017.09.030

German Aerospace Center. (2016). Global Urban Footprint. Retrieved October 31, 2018, from https://www.dlr.de/eoc/en/desktopdefault.aspx/tabid-9628/16557%7B%5C_%7Dread-40454/

Ghana Statistical Service. (2013). *2010 Population & Housing Census: Regional Analytical Report - Greater Accra Region.*

Ghana Statistical Service. (2014a). *2010 Population & Housing Census: Accra Metropolitan.*

Ghana Statistical Service. (2014b). *2010 Population & Housing Census: Ga South Municipality.* doi:10.1037/a0027164

Glanz, H., Carvalho, L., Sulla-Menashe, D., & Friedl, M. A. (2014). A parametric model for classifying land cover and evaluating training data based on multi-temporal remote sensing data. *ISPRS Journal of Photogrammetry and Remote Sensing*, *97*, 219–228. doi:10.1016/j.isprsjprs.2014.09.004

Gómez, C., White, J. C., & Wulder, M. A. (2016). Optical remotely sensed time series data for land cover classification: A review. *ISPRS Journal of Photogrammetry and Remote Sensing*. doi:10.1016/j.isprsjprs.2016.03.008

Gómez, C., White, J. C., Wulder, M. A., & Alejandro, P. (2014). Historical forest biomass dynamics modelled with Landsat spectral trajectories. *ISPRS Journal of Photogrammetry and Remote Sensing*, *93*, 14–28. doi:10.1016/j.isprsjprs.2014.03.008

Grant, R. & Yankson, P. (2003). Accra. *Cities*, *20*(1), 65–74. doi:10.1016/S0264-2751(02)00090-2

Hexagon AB. (2017). Using machine learning operators for raster and feature classification. Retrieved from https://community.hexagongeospatial.com/t5/ERDAS-IMAGINE/Machine-Learning-Raster-Classification/ta-p/23103

Homer, C., Dewitz, J., Yang, L., Jin, S., Danielson, P., Xian, G., ... Megown, K. (2015). Completion of the 2011 National Land Cover Database for the Conterminous United States – Representing a Decade of Land Cover Change Information. *Photogrammetric Engineering & Remote Sensing*, 345–354. doi:10.14358/PERS.81.5.345

Huang, J., Lu, X. X., & Sellers, J. M. (2007). A global comparative analysis of urban form: Applying spatial metrics and remote sensing. *Landscape and Urban Planning*, *82*(4), 184–197. doi:10.1016/j.landurbplan.2007.02.010

Huete, A., Didan, K., Miura, T., Rodriguez, E. P., Gao, X., & Ferreira, L. G. (2002). Overview of the radiometric and biophysical performance of the MODIS vegetation indices. *83*, 195–213.

Hussain, M., Chen, D., Cheng, A., Wei, H., & Stanley, D. (2013). Change detection from remotely sensed images: From pixel-based to object-based approaches. *ISPRS Journal of Photogrammetry and Remote Sensing*, *80*, 91–106. doi:10.1016/j.isprsjprs.2013.03.006

Jensen, J. R. (2005). *Introductory Digital Image Processing: A Remote Sensing Perspective* (3rd ed.).

Kassawmar, T., Eckert, S., Hurni, K., Zeleke, G., & Hurni, H. (2016). Reducing landscape heterogeneity for improved land use and land cover (LULC) classification across the large and complex Ethiopian highlands. *6049*(August). doi:10.1080/10106049.2016.1222637

Kondra, M. (2016). The status of the wetlands in the Greater Accra Region. (9). WaterPower Working Paper. Governance and Sustainability Lab. Trier.

Liu, D. & Xia, F. (2010). Assessing object-based classification: Advantages and limitations. *Remote Sensing Letters*, *1*(4), 187–194. doi:10.1080/01431161003743173

Liverman, D., Moran, E. F., Rindfuss, R. R., & Stern, P. C. (Eds.). (1998). *People and Pixels*. Washington, DC, USA: National Academies Press. doi:10.17226/5963

Manakos, I. & Lavender, S. (Eds.). (2014). *Land Use and Land Cover Mapping in Europe. Practices & Trends*. doi:10.1007/978-94-007-7969-3_1

Möller, M., Lymburner, L., & Volk, M. (2007). The comparison index: A tool for assessing the accuracy of image segmentation. *International Journal of Applied Earth Observation and Geoinformation*, *9*(3), 311–321. doi:10.1016/j.jag.2006.10.002

Myint, S. W., Gober, P., Brazel, A., Grossman-Clarke, S., & Weng, Q. (2011). Per-pixel vs. object-based classification of urban land cover extraction using high spatial resolution imagery. *Remote Sensing of Environment*, *115*(5), 1145–1161. doi:10.1016/j.rse.2010.12.017

Olofsson, P., Foody, G. M., Herold, M., Stehman, S. V., Woodcock, C. E., & Wulder, M. A. (2014). Good practices for estimating area and assessing accuracy of land change. *Remote Sensing of Environment*, *148*, 42–57. doi:10.1016/j.rse.2014.02.015

Pal, M. (2005). Random forest classifier for remote sensing classification. *International Journal of Remote Sensing*, *26*(1), 217–222. doi:10.1080/01431160412331269698

Pellow, D. N. (2007). *Resisting global toxics: the transnational movement for environmental justice*. Cambridge, MA: MIT Press.

Rindfuss, R. R. & Stern, P. C. (1998). Linking Remote Sensing and Social Science: The Need and the Challenges. In *People and pixels* (pp. 1–27).

Salem, M. (2016). Peri-urban dynamics and land-use planning for the Greater Cairo Region in Egypt. In C. A. Brebbia (Ed.), *Sustainable development* (Chap. Section 2: pp. 109–120). WIT Press.

Sartori, G. (1991). Comparing and miscomparing. *Journal of Theoretical Politics*, *3*(3), 243–257. doi:10.1177/0951692891003003001

Satellite Imaging Corporation. (2017a). QuickBird Satellite Sensor (0.65m) - Decommissioned. Retrieved July 9, 2018, from https://www.satimagingcorp.com/satellite-sensors/quickbird/

Satellite Imaging Corporation. (2017b). WorldView-2 Satellite Sensor (0.46m). Retrieved July 9, 2018, from https://www.satimagingcorp.com/satellite-sensors/worldview-2/

Seto, K. C., Woodcock, C. E., Song, C., Huang, X., Lu, J., & Kaufmann, R. K. (2002). Monitoring land-use change in the Pearl River Delta using Landsat TM. *International Journal of Remote Sensing*, *23*(10), 1985–2004. doi:10.1080/01431160110075532

Shackelford, A. K. & Davis, C. H. (2003). A combined fuzzy pixel-based and object-based approach for classification of high-resolution multispectral data over urban areas. *IEEE Transactions on Geoscience and Remote Sensing*, *41*(10 PART I), 2354–2363. doi:10.1109/TGRS.2003.815972

Silver, J. (2014). Incremental infrastructures: Material improvisation and social collaboration across post-colonial Accra. *Urban Geography*, *35*(6), 788–804. doi:10.1080/02723638.2014.933605

Simon, D., McGregor, D., & Nsiah Gyabaah, K. (2004). The changing urban-rural interface of African cities: Definitional issues and an application to Kumasi, Ghana. *Environment and Urbanization*, *16*(2), 235–248.

Simone, A. M. & Pieterse, E. (2017). *New urban worlds : inhabiting dissonant times*. Cambridge, Medford: Polity Press.

The Ramsar Convention Secretariat. (2014). Country profiles: Ghana. Retrieved July 20, 2018, from https://www.ramsar.org/wetland/ghana

The World Bank Group. (2015). *Rising through Cities in Ghana: Ghana urbanization review overview report*.

The World Bank Group. (2018). Country Historical Climate - Ghana. Retrieved July 20, 2018, from http://sdwebx.worldbank.org/climateportal/index.cfm

Tyroller, A. L. C. (2016). Changing Socio-Ecological Dynamics in an African Peri-Urban Wetland: The Case of the Fisheries in the Densu Delta Ramsar Site. (7). WaterPower Working Paper. Governance and Sustainability Lab, Trier University. Trier.

UN Habitat. (2014). *The State of African Cities: Re-imagining stustainable urban transitions*.

UN Habitat. (2016). *World Cities Report 2016 - Urbanization and Development: Emerging Futures*.

United Nations. (2016). *The World's Cities in 2016: Data Booklet*.

Vogelpohl, A. (2013). Qualitativ vergleichen – Zur komparativen Methodologie in Bezug auf räumliche Prozesse. In E. Rothfuß & T. Dörfler (Eds.), *Raumbezogene qualitative sozialforschung* (pp. 61–81). Wiesbaden: Springer VS. doi:10.1007/978-3-531-93240-8_3

Weable, C. (2018). *Analysis of two streets in the Densu Delta using Mapping Keys* (Doctoral dissertation, Trier University).

Xiuwan, C. (2002). Using remote sensing and GIS to analyse land cover change and its impacts on regional sustainable development. *International Journal of Remote Sensing*, *23*(1), 107–124. doi:10.1080/01431160010007051

Yankson, P. W. K. & Bertrand, M. (2012). Challenges of Urbanization in Ghana. In *The mobile city of accra: Urban families, housing and residential practices*.

A | Appendix

A.1 Overview of (Mosaic) Satellite Images

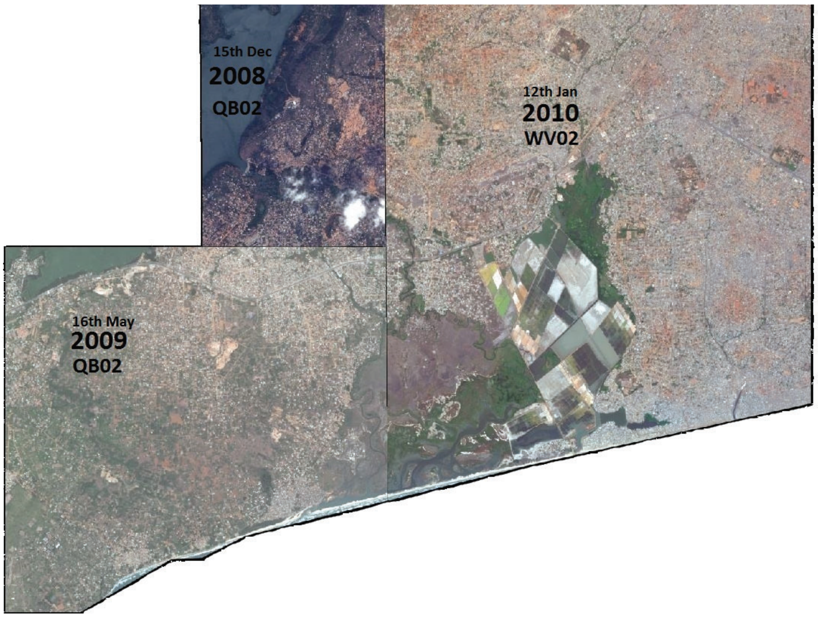

Figure A.1: Overview of the different satellite images used for 2008 till 2010: satellites and dates of recording

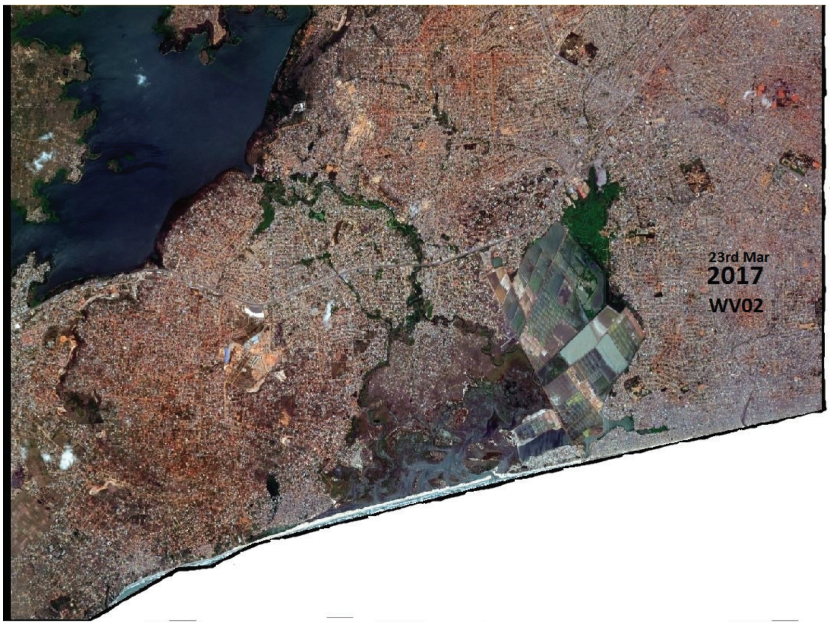

Figure A.2: Overview of the satellite image used for 2017: satellite and date of recording

A.2 Satellite Specifications

Table A.1: Sensor Bands WorldView-2 (Satellite Imaging Corporation, 2017b, 2017a)

	Bands	Wavelength
Panchromatic	Black/ White	450 - 800 nm
Multispectral	Coastal	400 - 450 nm
	Blue	450 - 510 nm
	Green	510 - 580 nm
	Yellow	585 - 625 nm
	Red	630 - 690 nm
	Red Edge	705 - 745 nm
	Near-IR1	770 - 895 nm
	Near-IR2	860 - 1040 nm

Table A.2: Sensor Bands QuickBird (Satellite Imaging Corporation, 2017b, 2017a)

	Bands	Wavelength
Panchromatic	Black/ White	405 - 1053 nm
Multispectral	Blue	430 - 545 nm
	Green	466 - 620 nm
	Red	590 - 710 nm
	Near-IR	715 - 918 nm

A.3 Change Detection

Since the classification of the class tarmac has an users accuracy of 41.2%, it is interesting to see, that streets are nonetheless visually recognizable, as shown in the figure below. This is one of the few instances in which a pattern is recognizable after the change detection (see table A.3).

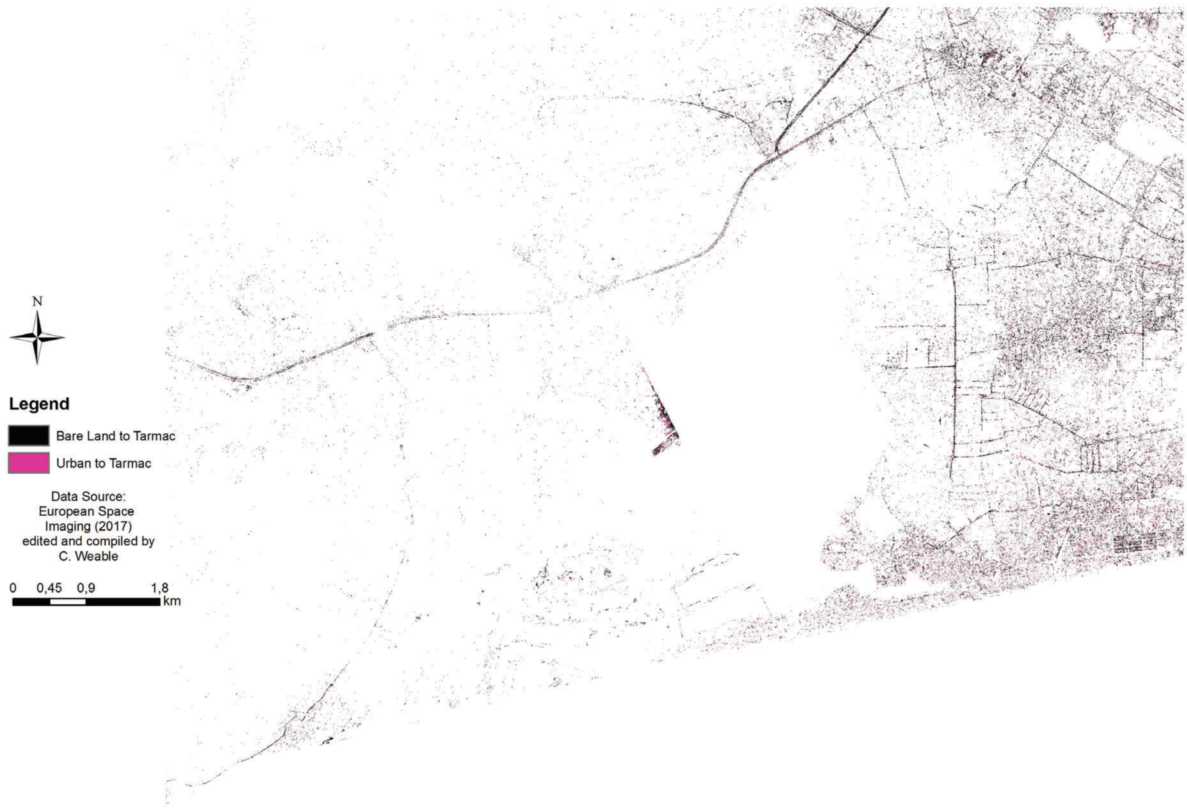

Figure A.3: Pixels which changed from 'Bare Land' and 'Urban' in 2008-2010 to 'Tarmac' in 2017

Table A.3: Land cover change pattern detection: change of class from 2008-2010 to 2017 and the visible results

	Class in 2008-2010	Class in 2017	Description and probable Causes
(I)	Bare Land (1)	Bare Land (1)	Areas inside the delta have a higher density and street patterns are recognizable; -
II	Bare Land (1)	Vegetation (2)	No patterns, mostly inside the delta and near the Weija lake; Vegetation change during seasons.
III	Bare Land (1)	Urban (3)	No pattern, slightly higher density inside the delta; geometric correction? General increase in urbanization and difficult class differentiation.
IV	Bare Land (1)	Tarmac (4)	Streets are recognizable, especially in AMA; Increase in tarmac streets over time in AMA
V	Bare Land (1)	Water (5)	No pattern, some scattered pixels along the coastline and near Weija lake;
VI	Vegetation (2)	Bare Land (1)	Higher density inside the delta and near West Hill Mall; Seasonal changes and a developing area near the Mall.
(VII)	Vegetation (2)	Vegetation (2)	Along the river, NE of delta and near Weija lake; -
VIII	Vegetation (2)	Urban (3)	Higher density in Ga South than AMA, especially Tetegu; Higher urban development in Ga South
IX	Vegetation (2)	Tarmac (4)	Only some scattered pixels, more inside the delta; wrongly classified.
X	Vegetation (2)	Water (5)	High density near Weija lake and inside the delta; Densu changed river course inside delta and Weija has a higher water level.
XI	Urban (3)	Bare Land (1)	No pattern to see, only slightly higher density in AMA; geometric correction?
XII	Urban (3)	Vegetation (2)	No pattern
(XIII)	Urban (3)	Urban (3)	Higher density in AMA, street patterns visible; -
XIV	Urban (3)	Tarmac (4)	Winneba Rd. and areas in AMA (e.g., Glefe); Asphalting and shadows
XV	Urban (3)	Water (5)	Predominantly in Glefe and surrounding areas; Urban shadows and high moisture in soil
XVI	Tarmac (4)	Bare Land (1)	Some in AMA; Tarmac mostly in AMA and due to sand and dirt being on the street
XVII	Tarmac (4)	Vegetation (2)	No pattern; -
XVIII	Tarmac (4)	Urban (3)	Main road; Cars and wrongly classified pixels
(XIX)	Tarmac (4)	Tarmac (4)	main road and some streets in AMA; -
XX	Tarmac (4)	Water (5)	Weija lake and Densu delta; problematic classification
XXI	Water (5)	Bare Land (1)	Delta area and coast; Change in water pathing
XXII	Water (5)	Vegetation (2)	Water bodies in NE of delta are gone and are now vegetated;
XXIII	Water (5)	Urban (3)	No pattern; Change of shade, etc.
XXIV	Water (5)	Tarmac (4)	No pattern; Difficult classification
(XXV)	Water (5)	Water (5)	Weija lake and Densu delta; -

WaterPower is a laboratory for experimenting with novel ways of doing research based on the integration of multiple disciplines, approaches, methods and non-academic knowledge through dialogue and collaboration.

We contribute to current debates on society-nature relations by mapping, analyzing and understanding processes that unfold in the urban water sphere.

Our analyses critically study the interplay of socio-political and ecological processes and how they configure place and scale.

WaterPower is funded by

SPONSORED BY THE

Federal Ministry of Education and Research

FONA
Research for Sustainable Development
BMBF

Governance and Sustainability Lab

Faculty VI - Regional and Environmental Sciences
Prof. Dr. Antje Bruns
University of Trier
www.uni-trier.de
www.waterpower.science